Research Square

Preprints are preliminary reports that have not undergone peer review.
They should not be considered conclusive, used to inform clinical practice,
or referenced by the media as validated information.

Fuzzy Hypergraph Consensus with Memory: A Novel $\boldsymbol{\alpha}$-Cut Spectral Framework for Uncertain Group Interactions with Applications to Social Interaction Networks

abdulkafi sanad

abdulkafisanad@stu.ynu.edu.cn

Yunnan University

Alhanouf M. Almutairi

Umm al-Qura University

Research Article

Keywords: Fuzzy hypergraph, Fuzzy Laplacian, α-cut, Fractional-order consensus, Robustness certificate, Uncertain group interactions

Posted Date: November 23rd, 2026

DOI: https://doi.org/10.21203/rs.3.rs-11709203/v1

License: This work is licensed under a Creative Commons Attribution 4.0 International License.
Read Full License

Additional Declarations: No competing interests reported.

RESEARCH

Fuzzy Hypergraph Consensus with Memory: A Novel α-Cut Spectral Framework for Uncertain Group Interactions with Applications to Social Interaction Networks

Abdulkafi Sanad[1,*] · **Alhanouf M. Almutairi**[2]

[*]Corresponding author: abdulkafisanad@stu.ynu.edu.cn

Abstract

Group interactions, graded relations and memory are inherent in real-world collective decision processes. Existing fuzzy graph and hypergraph models are static, while consensus models ignore the level structure of fuzzy information, so neither can certify how fast a group agrees or how robust this conclusion is. To bridge this gap, this paper introduces fractional-order fuzzy hypergraph consensus (FFHC), a unified framework that integrates fuzzy memberships, uniform hypergraphs and Caputo fractional dynamics through the fuzzy Laplacian $L_\mu = \sum_e \mu(e)(kI_e - \mathbf{1}_e\mathbf{1}_e^\top)$. An exact α-cut resolution of L_μ, sharp spectral-radius bounds, localized and interval-valued stability results, Mittag-Leffler decay bounds and the optimality of fuzzy 2-designs are established. A decision-support algorithm (SPEC-FC) is developed that returns consensus-speed certificates, robustness ranges and a certified-optimal allocation of a membership budget. It is applied to two social systems. On the Davis Southern Women data, it certifies that cohesion survives the loss of any of 12 of 14 events, whereas the Weyl bound certifies none. On sensor-recorded group contacts among 317 high-school students, every crisp threshold above 0.0032 disconnects the structure while the fuzzy model stays connected, and the optimal allocation, certified within 0.64% of optimality, raises the algebraic connectivity 12-fold. Statistical validation over 100 perturbation trials shows a coefficient of variation of at most 1.13% and perturbation bounds 4 to 30 times sharper than Weyl's. Future research directions include non-uniform hypergraphs, heterogeneous memory and learning-based membership estimation.

Keywords Fuzzy hypergraph · Fuzzy Laplacian · α-cut · Fractional-order consensus · Robustness certificate · Uncertain group interactions

Mathematics Subject Classification 05C65 · 05C50 · 03E72 · 26A33 · 34A08 · 15A42

1 Introduction

Decision-making in social, organizational and engineering systems is rarely a matter of isolated pairs. A committee meeting, a classroom, a project team or a social event involves several participants at once, and models that reduce such interactions to pairwise links can misrepresent both the structure and the behaviour of the system [1]. In practice, the information about these group relations is also uncertain. The strength of a group relation is inferred from incomplete records or assessed by experts, so it holds only to a degree, and this degree is revised when records are corrected or judgments are updated.

Fuzzy set theory [2] supplies the natural language for graded relations, and fuzzy hypergraphs [3] represent graded higher-order structure directly. Fuzzy graph models have proven effective for decision problems in which vagueness plays a central role [4, 5, 6]. Nonetheless, conventional fuzzy graph and hypergraph models remain essentially static. They do not describe how agreement forms over the structure, they do not capture memory effects, and they do not quantify how their conclusions change when memberships are revised.

Recent developments in fractional calculus and spectral hypergraph theory offer a way to address these limitations. Fractional operators model long-memory and hereditary dynamics [7, 8], while hypergraph Laplacians encode multi-way relations in a matrix whose spectrum governs diffusion and consensus [9, 10]. Building upon these paradigms, we introduce the *fractional-order fuzzy hypergraph consensus* (FFHC) framework. It unifies fuzzy memberships, higher-order structure and fractional-order dynamics, and it turns the defining features of fuzzy information (level sets, bounded memberships, interval uncertainty) into computable guarantees.

The present study develops the theoretical foundations of the framework, assembles them into a decision-support algorithm (SPEC-FC), and applies it to two real social systems: the Davis Southern Women affiliation data and sensor-recorded group contacts among high-school students [11]. The applications show that the framework certifies consensus speed, quantifies robustness to revised records and produces certified-optimal allocations of a limited membership budget.

1.1 Literature Review

The modelling of uncertain relational structure has drawn on fuzzy graphs, fuzzy hypergraphs, spectral graph theory and network dynamics, each of which contributes one ingredient of the present framework.

Fuzzy graphs, fuzzy hypergraphs and their extensions. Goetschel [3] introduced fuzzy hypergraphs and their level (α-cut) hypergraphs. Subsequent work extended the notion to q-rung orthopair [12], competition [13], soft competition [14] and spherical [15] fuzzy hypergraphs, mainly for decision-making, and domination has been studied for bipolar fuzzy graphs in several settings [4]. These contributions are combinatorial. They do not develop Laplacian spectra or dynamics.

Spectral models of fuzzy graphs. The Laplacian energy of a graph [16] has been transferred to picture fuzzy graphs [5] and to intuitionistic fuzzy rough graphs, where it supports energy-based decision-making [6]. These works concern pairwise relations and static spectral quantities. Stability under membership revision and the connection to dynamics are not considered.

Spectral theory of hypergraphs. Rodríguez [9, 17, 10] defined the hypergraph Laplacian through codegrees and related its eigenvalues to metric and partition parameters, and Banerjee [18] studied related operators. Cooper and Dutle [19], Qi [20] and Hu and Qi [21] developed tensor-based spectral theory, while nonlinear diffusion operators [22] and random-walk Laplacians [23] have been used for partitioning and learning [24]. All of these treat hyperedges as crisp or as carrying arbitrary weights.

Consensus, memory and spectral optimization. Consensus models for group decision-making account for trust among experts and for the unreliability of their opinions [25]. Cao et al. [7] established the coordination of networked fractional-order systems through the spectrum of the graph Laplacian, using the complete monotonicity of the Mittag-Leffler function [26, 8, 27, 28]. Maximizing the algebraic connectivity [29, 30] under a weight budget is a classical network-design problem [31, 32]. In these works the weights are not bounded by one and carry no level structure.

Table 1 compares these families of models with the proposed framework. While each family handles one or two of the four aspects, none handles all of them.

Table 1 Comparison of existing model families and the proposed FFHC framework.

Model family	Graded (fuzzy) relations	Higher-order (group) structure	Memory (fractional) dynamics	Computable guarantees
Fuzzy graphs and their energies [4, 5, 6]	Yes	No	No	No
Fuzzy hypergraphs [3, 12, 14]	Yes	Yes	No	No
Crisp hypergraph spectra [9, 18]	No	Yes	No	Partial
Fractional consensus on graphs [7]	No	No	Yes	Partial
Fuzzy consensus for group decisions [25]	Yes	No	No	No
FFHC (proposed)	Yes	Yes	Yes	Yes

Position of the proposed framework. The FFHC framework addresses this gap by:

- embedding uncertainty in a uniform hypergraph whose hyperedges carry membership degrees, so that group relations are represented without reduction to pairs;
- using the Caputo fractional derivative to encode memory in the consensus dynamics;
- exploiting the α-cuts, the bound $\mu \leq 1$ and interval-valued memberships to derive certificates that arbitrary weights do not admit.

The framework generalizes existing models: for $\mu \equiv 1$ the fuzzy Laplacian reduces to the codegree Laplacian of a crisp hypergraph [9], for $k = 2$ to the Laplacian of a fuzzy graph, and for $\beta = 1$ the dynamics reduce to ordinary consensus.

1.2 Recent Advances in Fuzzy Graph Models and Higher-Order Network Dynamics

Recent studies show a growing interest in spectral, higher-order and memory-aware models of uncertain systems. Five of them are closest to the present work.

- **Energies of picture fuzzy graphs:** Shi et al. [5] defined the Laplacian and skew Laplacian energies of picture fuzzy graphs and digraphs and derived bounds for them. Their work remains pairwise and static, and it does not consider revisions of the memberships.

- **Energy-based decision-making on intuitionistic fuzzy rough graphs:** Shaik and Shaik [6] combined similarity measures with Laplacian and signless Laplacian energies to rank alternatives. The model has no higher-order structure and no dynamics.
- **Trust-based consensus with unreliable opinions:** Tang et al. [25] proposed a consensus model that improves trust among experts while accounting for the unreliability of their hesitant fuzzy opinions. The interaction structure is pairwise and the process is memoryless.
- **Fractional higher-order networks:** Wang et al. [33] obtained synchronization criteria for short-memory fractional directed higher-order networks. The coupling weights are crisp, so the level structure of fuzzy information plays no role.
- **Spherical fuzzy hypergraphs:** Pramanik et al. [15] developed spherical fuzzy hypergraphs for decision-making. The treatment is combinatorial, without spectra, dynamics or robustness analysis.

Table 2 summarizes the scope of these studies relative to the proposed framework. None of them integrates graded memberships, higher-order structure, memory and certified robustness or optimality at the same time. This absence defines the research opportunity addressed here.

Table 2 Scope of recent studies relative to the proposed framework (✓: addressed; ×: not addressed).

Study	Fuzzy memberships	Higher-order structure	Fractional memory	Robustness certificates	Optimal allocation
Shi et al. (2022) [5]	✓	×	×	×	×
Tang et al. (2024) [25]	✓	×	×	×	×
Wang et al. (2025) [33]	×	✓	✓	×	×
Shaik and Shaik (2026) [6]	✓	×	×	×	×
Pramanik et al. (2026) [15]	✓	✓	×	×	×
Proposed FFHC	✓	✓	✓	✓	✓

1.3 Problem Formulation and Research Gap

Despite these advances, current approaches have three connected deficiencies.

1. **No transfer of fuzzy level structure to guarantees on consensus.** Existing consensus results [7, 33] use the spectrum of a crisp or arbitrarily weighted Laplacian. They provide no mechanism for turning the α-cuts of fuzzy information into guaranteed consensus speeds.
2. **No sharp account of membership revision.** Fuzzy memberships are revised or known only as intervals. Global Weyl-type estimates charge every revision in full. They distinguish neither localized from dispersed revisions nor increases from decreases, and they give no exact eigenvalue ranges for interval-valued memberships.
3. **No theory of optimal graded allocation.** When a limited amount of membership (cohesion, reliability, trust) can be allocated to groups, it is not known which allocations make consensus fastest, nor whether graded allocations can outperform all-or-nothing ones.

These limitations matter in systems that simultaneously involve

- group interactions that cannot be reduced to pairs,
- graded and revisable information about the strength of each group,
- memory in the way agreement forms.

To illustrate the practical need, consider the students of a school whose face-to-face group contacts are recorded by wearable sensors for one week [11]. An analyst who wants to know how quickly information or agreement can spread among the students faces two difficulties at once. First, a triad of students that met once in a week and a triad that met a hundred times are both “groups”, but to very different degrees. A crisp model must choose a threshold, and Section 8 shows that every threshold above 0.0032 disconnects the school, so that a crisp model predicts that agreement is impossible. Secondly, the record itself is uncertain. Had one recording day been lost, almost every membership would change. The analyst therefore needs to know which conclusions survive such a revision. A model based only on fuzzy sets can represent the degrees but says nothing about dynamics or robustness, whereas a consensus model with crisp weights describes the dynamics but ignores the graded and revisable nature of the data. The FFHC framework is designed for this dual requirement.

1.4 Justification for the Proposed Framework

The framework rests on one structural fact. The fuzzy Laplacian

$$L_\mu = \sum_{e\in E} \mu(e)\big(kI_e - \mathbf{1}_e\mathbf{1}_e^\top\big)$$

depends linearly on the memberships, and the solution of the Caputo consensus system ${}^{C}D_t^{\beta} x(t) = -L_\mu x(t)$, $0 < \beta \le 1$, is governed by the Mittag-Leffler function $E_\beta(-\lambda t^\beta)$, which is completely monotone in λ. Consequently, every lower bound on $\lambda_2(L_\mu)$ becomes a guaranteed decay rate, every Loewner comparison of memberships becomes a comparison of decay curves, and every optimal membership allocation for λ_2 is optimal for consensus simultaneously for all β and all t. For $\beta < 1$ the disagreement decays like $t^{-\beta}$ rather than exponentially, so the spectral quantities control the constant of an algebraic law. Fuzzy information and memory therefore fit together naturally, and the spectral theory of L_μ is the single tool that serves all three questions of the previous subsection.

1.5 Contributions

The main contributions of this research are summarized below. Results that follow directly from classical matrix theory are identified as such in the text.

1. **Formulation of the FFHC framework:** We introduce fractional-order consensus on fuzzy-weighted uniform hypergraphs, which integrates fuzzy memberships, higher-order structure and Caputo memory in one model.
2. **Theoretical development:** We prove an exact α-cut resolution $L_\mu = \int_0^1 L(H_\alpha)\,\mathrm{d}\alpha$ (Theorem 4) with level-averaged spectral bounds (Theorem 5); the sharp estimate $(k-1)d_{\max}(\mu) < \lambda_{\max}(L_\mu) \le k\,d_{\max}(\mu)$ (Theorem 2); a budget bound attained exactly by fuzzy 2-designs (Theorem 6); localized, one-sided and interval-valued stability results (Theorems 7–10); two-sided Mittag-Leffler decay bounds, certificates and trajectory stability (Theorems 11–13); and a characterization of optimal allocations (Theorems 14–16, Corollaries 2 and 3).
3. **Decision-support algorithm (SPEC-FC):** Algorithm 1 takes raw group observations and returns spectral diagnostics, consensus-speed certificates, robustness ranges and a certified-optimal membership allocation.
4. **Case study applications:** The framework is applied to the Davis Southern Women affiliation data and to sensor-recorded group contacts among 317 high-school students, where graded memberships keep a structure connected that every crisp threshold and every crisp allocation disconnects.
5. **Computational, comparative and statistical analysis:** We give a complexity analysis, compare the framework with six crisp, weighted and pairwise models, validate it statistically over repeated perturbation trials and report sensitivity analyses.
6. **Future research directions:** The limitations of the framework are stated explicitly, and extensions to non-uniform structures, heterogeneous memory and learning-based membership estimation are outlined.

1.6 Methodology

The methodology has four components, which correspond to the phases of Algorithm 1 (Fig. 1).

Fuzzy higher-order representation. Raw observations (attendance lists, timestamped group contacts) are converted into a k-uniform hypergraph. Each hyperedge receives a membership defined by a generalized Jaccard ratio, which is transparent, parameter-free and bounded by one. Leave-one-out deletions of the record define interval-valued memberships.

Spectral certificates. The α-cut resolution converts the level structure of the memberships into a lower bound on the algebraic connectivity. Load-based and one-sided perturbation bounds, together with an exact interval enclosure, quantify the effect of revisions.

Fractional-order dynamics. The Caputo derivative describes consensus with memory. The spectral certificates are transferred to the dynamics through the complete monotonicity of the Mittag-Leffler function, which yields guaranteed settling times.

Optimization with optimality certificates. The allocation of a membership budget is a concave program. It is solved by projected super-gradient ascent, and every iterate is accompanied by a weak-duality upper bound, so the user obtains a certified optimality gap rather than a heuristic answer.

1.7 Organization of the Article

The remainder of this paper is structured as follows. Section 2 introduces the preliminary concepts and the fuzzy-weighted hypergraph model. Section 3 develops the spectral theory of the fuzzy Laplacian and Section 4 the theory of fractional-

order consensus. Section 5 characterizes optimal membership allocations. Section 6 presents the SPEC-FC algorithm and its computational complexity. Sections 7 and 8 apply the framework to two real-world case studies. Section 9 gives a comparative analysis with existing models, Section 10 a statistical validation and Section 11 a sensitivity analysis. Section 12 discusses advantages and limitations. Finally, Section 13 concludes the paper and suggests directions for future research.

2 Preliminaries

This section presents the concepts and tools used throughout the paper. Only notions that are used later are introduced.

2.1 Fuzzy Sets, α-Cuts and Interval-Valued Memberships

Definition 1 ([2]) A fuzzy set $\tilde{A}$ on a finite universe X is given by a membership function $\mu_{\tilde{A}} : X \to [0,1]$. For $\alpha \in (0,1]$, its (weak) α-cut is $\tilde{A}_\alpha = \{x \in X : \mu_{\tilde{A}}(x) \geq \alpha\}$, and its support is $\operatorname{supp}\tilde{A} = \{x : \mu_{\tilde{A}}(x) > 0\}$.

The α-cuts are nested, i.e., $\alpha < \alpha'$ implies $\tilde{A}_{\alpha'} \subseteq \tilde{A}_\alpha$. The fuzzy set is recovered from them by the resolution identity [34], which we use in the integral form

$$\mu_{\tilde{A}}(x) = \int_0^1 \mathbf{1}\big[x \in \tilde{A}_\alpha\big]\, \mathrm{d}\alpha, \tag{1}$$

valid because the integrand equals 1 exactly for $\alpha \in (0, \mu_{\tilde{A}}(x)]$.

Definition 2 ([35]) An interval-valued fuzzy set on X assigns to each x a closed interval $[\mu^L(x), \mu^U(x)] \subseteq [0,1]$. A realization is any membership function μ with $\mu^L \leq \mu \leq \mu^U$ pointwise.

An intuitionistic fuzzy set [36] with membership μ and non-membership ν, $\mu + \nu \leq 1$, determines the interval $[\mu, 1-\nu]$. Hence all interval-valued results below apply to it as well.

2.2 Uniform Hypergraphs and Matrix Tools

Definition 3 A hypergraph $H = (V,E)$ has vertex set $V = \{1,\dots,n\}$ and a set E of m distinct subsets of V (hyperedges). It is k-uniform ($k \geq 2$) if $|e| = k$ for all $e \in E$. The incidence matrix $B \in \{0,1\}^{n\times m}$ has $B_{ve} = 1$ iff $v \in e$. The degree of v is $\deg(v)$, $\Delta(H) = \max_v \deg(v)$, the codegree of a pair $u \neq v$ is $c(u,v) = |\{e : \{u,v\} \subseteq e\}|$, and $c_2(H) = \max_{u\neq v} c(u,v)$. H is pair-balanced if $c(u,v)$ is constant; a pair-balanced k-uniform hypergraph with b hyperedges is a 2-(n,k,λ) design with $\lambda = bk(k-1)/(n(n-1))$, and the complete hypergraph $K_n^{(k)}$ is pair-balanced.

For a real symmetric matrix A, $\lambda_1(A) \leq \cdots \leq \lambda_n(A) = \lambda_{\max}(A)$ are its eigenvalues and $\lambda_j^{\downarrow}(A) = \lambda_{n-j+1}(A)$. $A \succeq 0$ means positive semidefinite (PSD), and $A \preceq B$ means $B - A \succeq 0$. We write $\mathbf{1}$ for the all-ones vector, $J = \mathbf{1}\mathbf{1}^\top$, $\mathbf{1}_e$ for the indicator vector of $e \subseteq V$, $I_e = \operatorname{diag}(\mathbf{1}_e)$, and x_e for the restriction of x to e. Norms are $\|x\|_1$, $\|x\|_\infty$ and $\|x\| = \|x\|_2$ for vectors, and $\|A\|_2 = \max_i |\lambda_i(A)|$ and $\|A\|_F = (\sum_{ij} A_{ij}^2)^{1/2}$ for symmetric matrices.

Definition 4 For symmetric A and $x \neq 0$, the Rayleigh quotient is $R_A(x) = x^\top Ax / x^\top x$. For a PSD matrix A with $A\mathbf{1} = 0$, the spectral radius is $\lambda_{\max}(A)$ and the algebraic connectivity (spectral gap) [29] is $\lambda_2(A)$.

Lemma 1 ([37, 38]) *Let A, B be real symmetric $n \times n$ matrices.*

(a) $\lambda_{\max}(A) = \max_{x\neq 0} R_A(x)$. *If $A \succeq 0$ and $A\mathbf{1} = 0$, then $\lambda_1(A) = 0$ and $\lambda_2(A) = \min\{R_A(x) : x \neq 0, x \perp \mathbf{1}\}$. A maximizing (minimizing) vector is an eigenvector.*

(b) (Weyl) $\lambda_i(A) + \lambda_1(B) \leq \lambda_i(A+B) \leq \lambda_i(A) + \lambda_{\max}(B)$; *in particular* $|\lambda_i(A) - \lambda_i(B)| \leq \|A - B\|_2$.

(c) If $A \preceq B$, then $\lambda_i(A) \leq \lambda_i(B)$ for all i.

(d) (Ky Fan) $\sum_{i\leq j} \lambda_i^{\downarrow}(A) = \max\{\operatorname{tr}(U^\top AU) : U \in \mathbb{R}^{n\times j}, U^\top U = I\}$; *consequently, the sum of any j diagonal entries of A is at most* $\sum_{i\leq j} \lambda_i^{\downarrow}(A)$.

Lemma 2 *For $0 < W \leq m$, the capped simplex $\mathscr{P}_W = \{x \in \mathbb{R}^m : 0 \leq x \leq \mathbf{1},\ \mathbf{1}^\top x = W\}$ is non-empty and compact, and $x \in \mathscr{P}_W$ is an extreme point if and only if at most one coordinate of x lies in $(0,1)$.*

Proof. If two coordinates satisfy $x_i, x_j \in (0,1)$, then $x \pm t(e_i - e_j) \in \mathscr{P}_W$ for small $t > 0$, so x is the midpoint of two distinct feasible points and is not extreme. Conversely, let x have at most one fractional coordinate and let $x = \frac{1}{2}(y+z)$ with $y, z \in \mathscr{P}_W$. Since $0 \leq y_i, z_i \leq 1$, every coordinate with $x_i \in \{0,1\}$ forces $y_i = z_i = x_i$. The constraint $\mathbf{1}^\top y = \mathbf{1}^\top z = W$ then fixes the remaining coordinate, so $y = z = x$. □

2.3 Fractional Calculus and the Mittag-Leffler Function

Definition 5 For $0<\beta<1$ and an absolutely continuous function f on $[0,T]$, the Caputo derivative of order β is

$$ {}^{C}D_t^{\beta} f(t) = \frac{1}{\Gamma(1-\beta)} \int_0^t (t-s)^{-\beta} f'(s)\,\mathrm{d}s, $$

and ${}^{C}D_t^{\beta} f = f'$ for $\beta = 1$. For vector-valued functions it acts componentwise.

Definition 6 The one-parameter Mittag-Leffler function is $E_\beta(z) = \sum_{j=0}^{\infty} \frac{z^j}{\Gamma(\beta j+1)}$, $\beta>0$, $z\in\mathbb{C}$. In particular $E_1(z) = e^z$.

Lemma 3 *Let $0<\beta\le 1$ and $g_\beta(z) = E_\beta(-z)$ for $z\ge 0$.*

(a) g_β is completely monotone on $[0,\infty)$ [26]. Hence $0<g_\beta(z)\le 1$, g_β is strictly decreasing, and $0\le -g_\beta'(z)\le 1/\Gamma(1+\beta)$ for all $z\ge 0$.

(b) For $0<\beta<1$ and $z\ge 0$ [27],

$$ \frac{1}{1+\Gamma(1-\beta)z} \;\le\; E_\beta(-z) \;\le\; \frac{1}{1+z/\Gamma(1+\beta)}, \tag{2} $$

and the upper bound also holds for $\beta = 1$.

(c) For $0<\beta<1$, $E_\beta(-z)\sim z^{-1}/\Gamma(1-\beta)$ as $z\to\infty$ [8].

Proof. (a) Complete monotonicity is Pollard's theorem for $\beta<1$, and it is obvious for $\beta=1$. A completely monotone function satisfies $(-1)^j g^{(j)}\ge 0$ for all j. Hence g_β is non-increasing and $-g_\beta'$ is a non-negative, non-increasing function. Consequently $-g_\beta'(z)\le -g_\beta'(0)$, and from the series, $-g_\beta'(0) = 1/\Gamma(\beta+1)$. Positivity follows from Bernstein's representation of g_β as the Laplace transform of a non-negative measure that is not identically zero. (b) is proved in [27]. For $\beta=1$ the upper bound reads $e^{-z}\le 1/(1+z)$. (c) is the classical algebraic tail of $E_\beta(-t^\beta)$, see [8]. □

Lemma 4 *Let $L\in\mathbb{R}^{n\times n}$ be symmetric PSD with spectral decomposition $L=\sum_{i=1}^n \lambda_i v_i v_i^{\top}$ and let $0<\beta\le 1$. The problem ${}^{C}D_t^{\beta} x(t) = -Lx(t)$, $x(0)=x_0$, has the unique continuous solution*

$$ x(t) = E_\beta(-Lt^\beta)x_0 = \sum_{i=1}^{n} E_\beta(-\lambda_i t^\beta)\,(v_i^{\top}x_0)\,v_i, \qquad t\ge 0. \tag{3} $$

Proof. In the orthonormal eigenbasis, $y_i(t) = v_i^{\top}x(t)$ satisfies the scalar problem ${}^{C}D_t^{\beta} y_i = -\lambda_i y_i$, $y_i(0) = v_i^{\top}x_0$. For $j\ge 1$, ${}^{C}D_t^{\beta} t^{\beta j} = \frac{\Gamma(\beta j+1)}{\Gamma(\beta(j-1)+1)} t^{\beta(j-1)}$, and ${}^{C}D_t^{\beta} 1 = 0$. The series $y_i(0)\sum_j (-\lambda_i)^j t^{\beta j}/\Gamma(\beta j+1)$ and the series of its term-wise Caputo derivatives converge uniformly on $[0,T]$ (they are dominated by $\sum_j (\lambda_i T^\beta)^j/\Gamma(\beta j+1)<\infty$), so term-wise differentiation is legitimate and gives ${}^{C}D_t^{\beta} y_i = -\lambda_i y_i$. For uniqueness, any continuous solution satisfies the Volterra equation $y(t) = y(0) - \frac{\lambda}{\Gamma(\beta)}\int_0^t (t-s)^{\beta-1} y(s)\,\mathrm{d}s$. If y,z are two solutions, then $w=y-z$ satisfies $|w(t)|\le \frac{\lambda}{\Gamma(\beta)}\int_0^t (t-s)^{\beta-1}|w(s)|\,\mathrm{d}s$. In the weighted norm $\|w\|_\theta = \sup_{t\le T} e^{-\theta t}|w(t)|$ this gives $\|w\|_\theta \le \lambda\,\theta^{-\beta}\|w\|_\theta$, because $\int_0^t (t-s)^{\beta-1}e^{-\theta(t-s)}\mathrm{d}s \le \Gamma(\beta)\theta^{-\beta}$. Choosing $\theta^\beta>\lambda$ yields $w\equiv 0$. □

2.4 Fuzzy-Weighted Uniform Hypergraphs

Definition 7 A fuzzy-weighted k-uniform hypergraph is a triple $\mathscr{H}_\mu = (V,E,\mu)$, where $H=(V,E)$ is k-uniform and $\mu: E\to[0,1]$ is a fuzzy hyperedge membership in the sense of Goetschel [3]. Its α-cut hypergraph is $H_\alpha = (V,E_\alpha)$ with $E_\alpha = \{e : \mu(e)\ge\alpha\}$, its support hypergraph is $H^+ = (V,E^+)$ with $E^+ = \{e:\mu(e)>0\}$, and its total membership is $W(\mu) = \sum_e \mu(e)$.

Definition 8 For $\mathscr{H}_\mu$ define the fuzzy degree $d_\mu(v) = \sum_{e\ni v}\mu(e)$, $d_{\max}(\mu) = \max_v d_\mu(v)$, the fuzzy codegree $a_\mu(u,v) = \sum_{e\supseteq\{u,v\}}\mu(e)$ $(u\ne v)$, $a_\mu(v,v)=0$, the fuzzy adjacency matrix $A_\mu = (a_\mu(u,v))$, the degree matrix $D_\mu = \operatorname{diag}\big(\sum_u a_\mu(v,u)\big)$, and the fuzzy Laplacian $L_\mu = D_\mu - A_\mu$. For one hyperedge put $L_e = kI_e - \mathbf{1}_e\mathbf{1}_e^{\top}$.

Proposition 1 *For every fuzzy-weighted k-uniform hypergraph:*

(i) $D_\mu = (k-1)\operatorname{diag}(d_\mu)$;

(ii) $L_\mu = \sum_e \mu(e)L_e = k\operatorname{diag}(d_\mu) - BM_\mu B^{\top}$, where $M_\mu = \operatorname{diag}(\mu(e))$;

(iii) $x^{\top}L_\mu x = \sum_e \mu(e)\sum_{\{u,v\}\subseteq e}(x_u-x_v)^2 = \sum_e \mu(e)\big(k\|x_e\|^2 - (\mathbf{1}_e^{\top}x)^2\big)$; hence $L_\mu\succeq 0$ and $L_\mu\mathbf{1}=0$;

(iv) $\operatorname{tr} L_\mu = k(k-1)W(\mu)$.

Proof. *Step 1 (degree matrix).* Fix v. Each hyperedge $e \ni v$ contributes $\mu(e)$ to exactly $k-1$ codegrees $a_\mu(v,u)$, $u \in e \setminus \{v\}$. Hence $\sum_u a_\mu(v,u) = (k-1)d_\mu(v)$, which is (i).

Step 2 (representations). L_e has diagonal entries $k-1$ on e and off-diagonal entries -1 on pairs inside e. Summing $\mu(e)L_e$ therefore gives the diagonal $(k-1)d_\mu(v)$ and the off-diagonal entries $-a_\mu(u,v)$, i.e., L_μ. Moreover, $(BM_\mu B^\top)_{uv} = \sum_e \mu(e)B_{ue}B_{ve}$ equals $a_\mu(u,v)$ if $u \neq v$ and $d_\mu(v)$ if $u = v$, so $k\operatorname{diag}(d_\mu) - BM_\mu B^\top$ has diagonal $(k-1)d_\mu$ and off-diagonal $-a_\mu$. This is (ii).

Step 3 (quadratic form). Lagrange's identity gives $k\|x_e\|^2 - (\mathbf{1}_e^\top x)^2 = \sum_{\{u,v\}\subseteq e}(x_u - x_v)^2 = x^\top L_e x$. Summing with the non-negative weights $\mu(e)$ gives (iii).

Step 4 (trace). $\operatorname{tr} L_e = k(k-1)$, so (iv) follows from (ii). □

Remark 1 Item (i) shows that the degree matrix of L_μ is $(k-1)\operatorname{diag}(d_\mu)$ and not $\operatorname{diag}(d_\mu)$. Using $\operatorname{diag}(d_\mu) - A_\mu$ would produce a matrix with row sums $-(k-2)d_\mu(v)$, which is not PSD for $k \geq 3$. If $\mu \equiv 1$, L_μ is the codegree Laplacian of Rodríguez [9]. For general μ it is the Laplacian of the weighted clique expansion with weights $a_\mu(u,v)$, so facts that depend only on this weighted-graph structure are inherited from graph theory. The results below use, in addition, the k-clique structure of the weights, the cap $\mu \leq 1$ and the α-cut structure of μ. Finally, $\mu(e)$ is a degree of membership in a fuzzy concept; it is neither a probability nor an unbounded importance weight.

Example 1 Let $k = 3$, $V = \{1,\ldots,5\}$, $e_1 = \{1,2,3\}$, $e_2 = \{3,4,5\}$, $e_3 = \{1,4,5\}$ and $\mu = (0.9, 0.6, 0.3)$. Then $d_\mu = (1.2, 0.9, 1.5, 0.9, 0.9)$, $W = 1.8$, and

$$L_\mu = \begin{pmatrix} 2.4 & -0.9 & -0.9 & -0.3 & -0.3 \\ -0.9 & 1.8 & -0.9 & 0 & 0 \\ -0.9 & -0.9 & 3.0 & -0.6 & -0.6 \\ -0.3 & 0 & -0.6 & 1.8 & -0.9 \\ -0.3 & 0 & -0.6 & -0.9 & 1.8 \end{pmatrix},$$

whose trace $10.8 = k(k-1)W$ agrees with Proposition 1(iv). Its spectrum is

$$\sigma(L_\mu) = \{0,\ 1.2055,\ 2.7000,\ 3.0940,\ 3.8005\}.$$

3 Spectral Theory of the Fuzzy Laplacian

This section develops the spectral properties of L_μ that are used for the fractional dynamics in Section 4. Each result is followed by its equality or limiting cases and a short interpretation.

3.1 Kernel and Spectral Radius

Theorem 1 *L_μ is symmetric and PSD. The multiplicity of its eigenvalue 0 equals the number of connected components of the support hypergraph H^+, isolated vertices included, and $\ker L_\mu$ is spanned by the indicator vectors of these components.*

Proof. By Proposition 1(iii), $x^\top L_\mu x$ is a sum of non-negative terms, so $L_\mu \succeq 0$. For a PSD matrix, $L_\mu x = 0$ iff $x^\top L_\mu x = 0$. The latter holds iff $x_u = x_v$ whenever u, v lie in a common hyperedge of positive membership, i.e., iff x is constant on every component of H^+. □

Corollary 1 *$\lambda_2(L_\mu) > 0$ if and only if H^+ is connected; in particular, connectivity of any α-cut H_α implies $\lambda_2(L_\mu) > 0$.*

Remark 2 Theorem 1 is the fuzzy-hypergraph form of a standard weighted-graph fact. Its precise formulation matters, however. The statement "$\ker L_\mu$ corresponds to the components of H" is false: if two disjoint hyperedges are joined by a third with membership 0, then H is connected but $\lambda_2(L_\mu) = 0$. Connectivity of a fuzzy hypergraph is a property of its support.

Theorem 2 *Let $\mu \not\equiv 0$ and $V_{\max} = \{v : d_\mu(v) = d_{\max}(\mu)\}$. Then*

$$(k-1)\, d_{\max}(\mu) < \lambda_{\max}(L_\mu) \leq k\, d_{\max}(\mu), \tag{4}$$

and the upper bound is attained if and only if there exists $x \neq 0$ with

$$\operatorname{supp}(x) \subseteq V_{\max} \quad \text{and} \quad \mathbf{1}_e^\top x = 0 \ \text{ for all } e \in E^+. \tag{5}$$

Proof. *Step 1 (upper bound).* By Proposition 1(iii), for every x,

$$x^\top L_\mu x = \sum_e \mu(e)\big(k\|x_e\|^2 - (\mathbf{1}_e^\top x)^2\big) \leq k\sum_e \mu(e)\|x_e\|^2 = k\sum_v d_\mu(v)x_v^2 \leq k\, d_{\max}(\mu)\|x\|^2, \tag{6}$$

where the equality in the middle regroups $\sum_e \mu(e)\sum_{v\in e} x_v^2$ by vertices. Lemma 1(a) gives $\lambda_{\max}(L_\mu) \le k\, d_{\max}(\mu)$.

Step 2 (equality). If $x \neq 0$ satisfies (5), both inequalities in (6) are equalities, so $R_{L_\mu}(x) = k\, d_{\max}(\mu)$. Conversely, if $\lambda_{\max}(L_\mu) = k\, d_{\max}(\mu)$, let x be a corresponding eigenvector. Equality in the first inequality of (6) forces $\mu(e)(\mathbf{1}_e^\top x)^2 = 0$ for all e. Equality in the second forces $(d_{\max} - d_\mu(v))x_v^2 = 0$ for all v. Together these are (5).

Step 3 (strict lower bound). For $v \in V_{\max}$, $R_{L_\mu}(e_v) = (L_\mu)_{vv} = (k-1)d_{\max}(\mu)$ by Proposition 1(i), so $\lambda_{\max} \ge (k-1)d_{\max}$. If equality held, e_v would be an eigenvector (Lemma 1(a)). Then column v of L_μ would vanish off the diagonal, i.e., $a_\mu(u,v) = 0$ for all $u \neq v$. This contradicts $\sum_u a_\mu(u,v) = (k-1)d_\mu(v) > 0$. □

Second proof of the upper bound. By Proposition 1(ii),

$$k\,\mathrm{diag}(d_\mu) - L_\mu = (BM_\mu^{1/2})(BM_\mu^{1/2})^\top \succeq 0.$$

Hence $L_\mu \preceq k\,\mathrm{diag}(d_\mu) \preceq k\, d_{\max}(\mu) I$, and Lemma 1(c) applies.

Remark 3 (Equality and limiting cases) (a) For $k = 2$, (5) is the classical condition for $\lambda_{\max} = 2\Delta$ (a bipartite component with all degrees maximal). (b) The bound is attained on non-complete hypergraphs. For a single hyperedge, $\lambda_{\max} = k\mu(e)$. For the cyclic 3-uniform hypergraph with edges $\{i, i+1, i+2\} \bmod n$, $3 \mid n$, and constant membership t, the vector $(1,-1,0,1,-1,0,\dots)$ satisfies (5), so $\lambda_{\max} = 9t$. (c) For $K_n^{(k)}$ with $n > k$ and $\mu \equiv t$, $L_\mu = t\binom{n-2}{k-2}(nI - J)$. Thus $\lambda_{\max} = tn\binom{n-2}{k-2} < k\, d_{\max} = t\frac{k(n-1)}{k-1}\binom{n-2}{k-2}$. (d) Gershgorin's theorem gives only $\lambda_{\max} \le 2(k-1)d_{\max}$, which is weaker for every $k \ge 3$.

Theorem 3 *For every $j = 1,\dots,n$, with fuzzy degrees ordered as $d_{[1]} \ge \cdots \ge d_{[n]}$,*

$$\lambda_j^{\downarrow}(L_\mu) \le k\, d_{[j]} \qquad \text{and} \qquad (k-1)\sum_{i\le j} d_{[i]} \le \sum_{i\le j} \lambda_i^{\downarrow}(L_\mu) \le k \sum_{i\le j} d_{[i]}.$$

Proof. $L_\mu \preceq k\,\mathrm{diag}(d_\mu)$ (second proof of Theorem 2) and Lemma 1(c) give $\lambda_j^{\downarrow}(L_\mu) \le k d_{[j]}$; summing gives the right inequality. The diagonal of L_μ is $(k-1)d_\mu$, and Lemma 1(d) gives the left inequality. □

3.2 The α-Cut Resolution

Let $0 = \alpha_0 < \alpha_1 < \cdots < \alpha_r \le 1$, where $\alpha_1,\dots,\alpha_r$ are the distinct positive values of μ, and let $L(H_\alpha)$ denote the crisp Laplacian of H_α.

Theorem 4 *For every fuzzy-weighted k-uniform hypergraph,*

$$L_\mu = \int_0^1 L(H_\alpha)\,\mathrm{d}\alpha = \sum_{j=1}^{r} (\alpha_j - \alpha_{j-1})\, L(H_{\alpha_j}), \qquad L(H_{\alpha_r}) \preceq \cdots \preceq L(H_{\alpha_1}) = L(H^+). \tag{7}$$

Proof. *Step 1.* By (1), $\mu(e) = \int_0^1 \mathbf{1}[e \in E_\alpha]\,\mathrm{d}\alpha$. Inserting this into $L_\mu = \sum_e \mu(e) L_e$ and exchanging the finite sum and the integral gives $L_\mu = \int_0^1 \sum_{e\in E_\alpha} L_e\,\mathrm{d}\alpha = \int_0^1 L(H_\alpha)\,\mathrm{d}\alpha$. *Step 2.* For $\alpha \in (\alpha_{j-1}, \alpha_j]$, $E_\alpha = E_{\alpha_j}$, and $E_\alpha = \emptyset$ for $\alpha > \alpha_r$; this gives the finite sum. *Step 3.* If $\alpha < \alpha'$, then $L(H_\alpha) - L(H_{\alpha'}) = \sum_{e\in E_\alpha \setminus E_{\alpha'}} L_e \succeq 0$. *Independent check.* The coefficient of L_e on the right of (7) for a hyperedge with $\mu(e) = \alpha_p$ is $\sum_{j\le p}(\alpha_j - \alpha_{j-1}) = \alpha_p$ (telescoping). □

Theorem 5 *With the notation of Theorem 4,*

$$\lambda_2(L_\mu) \ge \gamma_\alpha(\mu) = \sum_{j=1}^{r} (\alpha_j - \alpha_{j-1})\, \lambda_2(L(H_{\alpha_j})) \;\ge\; \max_j \alpha_j\, \lambda_2(L(H_{\alpha_j})), \tag{8}$$

$$\lambda_{\max}(L_\mu) \le \sum_{j=1}^{r} (\alpha_j - \alpha_{j-1})\, \lambda_{\max}(L(H_{\alpha_j})). \tag{9}$$

Proof. *Step 1.* All $L(H_{\alpha_j})$ are PSD with $\mathbf{1}$ in their kernels. For every unit $x \perp \mathbf{1}$, (7) gives $x^\top L_\mu x = \sum_j (\alpha_j - \alpha_{j-1}) x^\top L(H_{\alpha_j}) x \ge \gamma_\alpha(\mu)$. Minimizing over x (Lemma 1(a)) yields the first inequality. *Step 2.* By the Loewner chain and Lemma 1(c), $\lambda_2(L(H_{\alpha_i})) \ge \lambda_2(L(H_{\alpha_j}))$ for $i \le j$. Dropping the terms $i > j$ gives $\gamma_\alpha(\mu) \ge \sum_{i\le j}(\alpha_i - \alpha_{i-1})\lambda_2(L(H_{\alpha_j})) = \alpha_j \lambda_2(L(H_{\alpha_j}))$ for every j. *Step 3.* For every unit x, $x^\top L_\mu x \le \sum_j (\alpha_j - \alpha_{j-1})\lambda_{\max}(L(H_{\alpha_j}))$, which is (9). □

Remark 4 The usual transfer of a crisp bound, $L_\mu \succeq \mu_{\min}^+ L(H^+)$, gives $\lambda_2(L_\mu) \ge \mu_{\min}^+ \lambda_2(L(H^+))$. This is the term $j = 1$ of the maximum in (8), so the α-cut bound is never worse; Section 9 shows that it is typically much better. For constant μ all three quantities coincide. Interpretation: the algebraic connectivity of a fuzzy hypergraph is at least the *level-averaged* connectivity of its crisp α-cuts, each weighted by the length of the confidence interval on which that cut is valid.

Example 2 (Example 1 continued) The α-cut spectra are $\{0,2,5,5,6\}$ ($\alpha = 0.3$), $\{0,1,3,3,5\}$ ($\alpha = 0.6$) and $\{0,0,0,3,3\}$ ($\alpha = 0.9$). Hence $\gamma_\alpha = 0.3(2+1+0) = 0.9$, whereas $\mu_{\min}\lambda_2(L(H)) = 0.6$ (true value 1.2055). Likewise, (9) gives $\lambda_{\max} \le 4.2$, sharper than $k\, d_{\max} = 4.5$ (true value 3.8005). Here $V_{\max} = \{3\}$, so (5) fails and $3.0 < 3.8005 < 4.5$ strictly.

3.3 A Budget Bound

Theorem 6 *For every fuzzy-weighted k-uniform hypergraph on $n \geq 2$ vertices with total membership W,*

$$\lambda_2(L_\mu) \leq \frac{k(k-1)W}{n-1} \leq \lambda_{\max}(L_\mu), \tag{10}$$

and equality holds in either inequality if and only if μ is a fuzzy 2-design, i.e., $a_\mu(u,v) = \frac{k(k-1)W}{n(n-1)}$ for all $u \neq v$. In that case $L_\mu = \frac{k(k-1)W}{n-1}(I - \frac{1}{n}J)$.

Proof. *Step 1.* $\lambda_1 = 0$ and $\sum_{i\geq 2}\lambda_i = \operatorname{tr} L_\mu = k(k-1)W$ (Proposition 1). The smallest of $\lambda_2, \ldots, \lambda_n$ is at most their mean $c = k(k-1)W/(n-1)$, and the largest is at least c. *Step 2.* Equality forces $\lambda_2 = \cdots = \lambda_n = c$. Since $\mathbf{1}$ spans the kernel, $L_\mu = c(I - J/n)$. Comparing off-diagonal entries gives $a_\mu(u,v) = c/n$. Conversely, a constant codegree together with zero row sums gives $L_\mu = c(I - J/n)$. □

3.4 Stability under Membership Uncertainty

Let μ, ν be two membership functions, $\delta = \mu - \nu$, and define the *maximum vertex load*

$$\ell(\delta) = \max_v \sum_{e \ni v} |\delta(e)| = d_{\max}(|\delta|).$$

Pointwise $|\delta|$, $\mu \wedge \nu$, $\mu \vee \nu$ and $(\nu - \mu)_+$ are again membership functions. This closure property is specific to $[0,1]$-valued memberships.

Lemma 5 $L_\mu - L_\nu = \sum_e \delta(e) L_e$ *and* $-L_{|\delta|} \preceq L_\mu - L_\nu \preceq L_{|\delta|}$. *Moreover* $\|L_e\|_2 = k$, $\|L_e\|_F = k\sqrt{k-1}$, *and*

$$\|L_\mu - L_\nu\|_2 \leq \lambda_{\max}(L_{|\delta|}) \leq k\,\ell(\delta) \leq k\|\delta\|_1.$$

Proof. The identity is linearity. Since $L_e \succeq 0$, the matrices $L_{|\delta|} \mp \sum_e \delta(e) L_e = \sum_e (|\delta(e)| \mp \delta(e)) L_e$ are PSD. L_e has eigenvalue k with multiplicity $k-1$ and 0 otherwise, which gives both norms. The chain of inequalities follows from the Loewner sandwich, from Theorem 2 applied to $|\delta|$, and from $\ell(\delta) \leq \|\delta\|_1$. □

The bound $|\lambda_i(L_\mu) - \lambda_i(L_\nu)| \leq k\|\delta\|_1$ (Weyl) is standard. The next results refine it.

Theorem 7 *For every i, $\lambda_i(L_{\mu\wedge\nu}) \leq \lambda_i(L_\mu), \lambda_i(L_\nu) \leq \lambda_i(L_{\mu\vee\nu})$, and*

$$|\lambda_i(L_\mu) - \lambda_i(L_\nu)| \leq \lambda_{\max}(L_{|\delta|}) \leq k\,\ell(\delta) \leq k \min\{\|\delta\|_1,\ \Delta(H^\delta)\|\delta\|_\infty\},$$

where $H^\delta = (V, \operatorname{supp}\delta)$. All inequalities are attained when δ is supported on one hyperedge.

Proof. *Step 1.* $\mu \wedge \nu \leq \mu, \nu \leq \mu \vee \nu$ pointwise, and L is Loewner-monotone in the membership (Theorem 9), which gives the sandwich. *Step 2.* $\mu \vee \nu - \mu \wedge \nu = |\delta|$, so by Weyl's inequality the sandwich interval has length at most $\lambda_{\max}(L_{|\delta|})$. *Step 3.* The remaining inequalities are Lemma 5 together with $\sum_{e\ni v}|\delta(e)| \leq \|\delta\|_\infty \Delta(H^\delta)$. *Step 4 (sharpness).* For $\nu \equiv 0$ and $\mu = t\mathbf{1}_{\{e_0\}}$, all quantities equal kt. □

Theorem 8 *For any μ, ν: $\lambda_2(L_\mu) \geq \lambda_2(L_{\mu\wedge\nu}) \geq \lambda_2(L_\nu) - \lambda_{\max}(L_{(\nu-\mu)_+}) \geq \lambda_2(L_\nu) - k\,\ell((\nu-\mu)_+)$. Consequently, increases of membership never decrease λ_2, and the support of μ is connected whenever $k\,\ell((\nu-\mu)_+) < \lambda_2(L_\nu)$.*

Proof. The first inequality is monotonicity. Since $\mu \wedge \nu = \nu - (\nu - \mu)_+$, Weyl's inequality gives the second. The third is Theorem 2 applied to $(\nu - \mu)_+$. □

Theorem 9 *If $\mu \leq \nu$ pointwise, then $L_\mu \preceq L_\nu$ and $\lambda_i(L_\mu) \leq \lambda_i(L_\nu)$ for all i.*

Proof. $L_\nu - L_\mu = \sum_e (\nu(e) - \mu(e)) L_e \succeq 0$; apply Lemma 1(c). □

Theorem 10 *For interval-valued memberships $[\mu^L, \mu^U]$ with realization set $\mathscr{R}$ and every i, $\{\lambda_i(L_\mu) : \mu \in \mathscr{R}\} = [\lambda_i(L_{\mu^L}), \lambda_i(L_{\mu^U})]$.*

Proof. Theorem 9 gives the inclusion "$\subseteq$", and the endpoints are attained at μ^L and μ^U. The map $\mu \mapsto \lambda_i(L_\mu)$ is continuous (Lemma 5) and $\mathscr{R}$ is convex, so the image is an interval. □

Remark 5 For general symmetric interval matrices, extreme eigenvalue ranges require up to 2^{n-1} vertex evaluations [39]. Theorem 10 shows that interval-valued fuzzy hyperedge memberships form a structured subclass in which *every* eigenvalue range is exact after two eigen-decompositions, because uncertainty enters only through non-negative multiples of the PSD matrices L_e.

Table 3 summarizes the properties established in this section.

Table 3 Summary of the spectral properties of the fuzzy Laplacian L_μ and their status.

Property	Statement	Relation to classical results
PSD, kernel	0-multiplicity = components of H^+ (Theorem 1)	classical (weighted graphs)
Spectral radius	$(k-1)d_{\max} < \lambda_{\max} \le k d_{\max}$, equality characterized (Theorem 2)	refined
Majorization	$\lambda_j^{\downarrow} \le k d_{[j]}$, two-sided partial sums (Theorem 3)	refined
α-cut resolution	$L_\mu = \int_0^1 L(H_\alpha)\mathrm{d}\alpha$ (Theorem 4)	fuzzy-specific
α-cut bounds	level-averaged λ_2, $\lambda_{\max}$ bounds (Theorem 5)	fuzzy-specific
Budget bound	$\lambda_2 \le k(k-1)W/(n-1)$, fuzzy 2-designs (Theorem 6)	refined
Localized stability	shift $\le k\,\ell(\delta)$ (Theorem 7)	refined
One-sided gap stability	only losses matter (Theorem 8)	fuzzy-specific
Interval enclosure	exact eigenvalue ranges (Theorem 10)	fuzzy-specific

4 Fractional-Order Consensus on Fuzzy Hypergraphs

Definition 9 Let $\mathscr{H}_\mu$ be a fuzzy-weighted k-uniform hypergraph and $0 < \beta \le 1$. The *fractional-order fuzzy hypergraph consensus* (FFHC) system is

$$ {}^{C}D_t^{\beta} x(t) = -L_\mu x(t), \qquad x(0) = x_0 \in \mathbb{R}^n, \qquad t \ge 0, \tag{11}$$

or, componentwise, ${}^{C}D_t^{\beta} x_v(t) = -\sum_{e \ni v} \mu(e) \sum_{u \in e} \big(x_v(t) - x_u(t)\big)$.

Each agent v relaxes towards the members of every group e to which it belongs, with strength $\mu(e)$. The Caputo derivative makes the relaxation depend on the whole history of x_v, with a power-law memory kernel of exponent $-\beta$. For $\beta = 1$ the system is the classical (memoryless) consensus. Let $\bar{x} = \frac{1}{n}\mathbf{1}^\top x_0$ and $e(t) = x(t) - \bar{x}\mathbf{1}$ denote the disagreement vector.

Theorem 11 *Let $x(t)$ solve (11), and write $\lambda_2 = \lambda_2(L_\mu)$ and $\lambda_{\max} = \lambda_{\max}(L_\mu)$.*

(i) (Conservation) For every connected component C of H^+, $\sum_{v \in C} x_v(t)$ is constant in t.

(ii) (Limit) $x(t) \to P x_0$ as $t \to \infty$, where P is the orthogonal projector onto $\ker L_\mu$ (component-wise averaging).

(iii) (Two-sided decay) If H^+ is connected, then for all $t \ge 0$

$$ E_\beta(-\lambda_{\max} t^\beta)\,\|e(0)\| \;\le\; \|e(t)\| \;\le\; E_\beta(-\lambda_2 t^\beta)\,\|e(0)\|, \tag{12}$$

both bounds are attained (by eigenvectors of $\lambda_{\max}$ and λ_2), and $t \mapsto \|e(t)\|$ is non-increasing.

(iv) (Algebraic law) If H^+ is connected and $0 < \beta < 1$, then

$$ \frac{\|e(0)\|}{1 + \Gamma(1-\beta)\lambda_{\max} t^\beta} \le \|e(t)\| \le \frac{\|e(0)\|}{1 + \lambda_2 t^\beta / \Gamma(1+\beta)}. \tag{13}$$

In particular, $\liminf_{t\to\infty} t^\beta \|e(t)\| \ge \|e(0)\|/(\Gamma(1-\beta)\lambda_{\max}) > 0$ for $e(0) \ne 0$: fractional consensus on a fuzzy hypergraph is never exponential when $\beta < 1$.

Proof. Let $L_\mu = \sum_i \lambda_i v_i v_i^\top$ with $0 = \lambda_1 \le \cdots \le \lambda_n$. By Lemma 4, $x(t) = \sum_i E_\beta(-\lambda_i t^\beta) c_i v_i$ with $c_i = v_i^\top x_0$.

Step 1 (i). By Theorem 1, the indicator $\mathbf{1}_C$ of a component lies in $\ker L_\mu$. Hence $\mathbf{1}_C^\top x(t) = \sum_i E_\beta(-\lambda_i t^\beta) c_i \mathbf{1}_C^\top v_i$. For $\lambda_i > 0$, $v_i \perp \ker L_\mu$, so $\mathbf{1}_C^\top v_i = 0$; for $\lambda_i = 0$, $E_\beta(0) = 1$. Therefore $\mathbf{1}_C^\top x(t) = \mathbf{1}_C^\top x_0$.

Step 2 (ii). For $\lambda_i > 0$, $E_\beta(-\lambda_i t^\beta) \to 0$ as $t \to \infty$ by Lemma 3(b),(c) (and $e^{-\lambda_i t} \to 0$ for $\beta = 1$). The kernel components are preserved, so $x(t) \to \sum_{\lambda_i = 0} c_i v_i = P x_0$.

Step 3 (iii). If H^+ is connected, $v_1 = \mathbf{1}/\sqrt{n}$ and $e(t) = \sum_{i \ge 2} E_\beta(-\lambda_i t^\beta) c_i v_i$. By Lemma 3(a), $s \mapsto E_\beta(-s t^\beta)$ is non-increasing, so $E_\beta(-\lambda_{\max} t^\beta) \le E_\beta(-\lambda_i t^\beta) \le E_\beta(-\lambda_2 t^\beta)$ for $i \ge 2$. Hence $\|e(t)\|^2 = \sum_{i \ge 2} E_\beta(-\lambda_i t^\beta)^2 c_i^2$ lies between $E_\beta(-\lambda_{\max} t^\beta)^2 \|e(0)\|^2$ and $E_\beta(-\lambda_2 t^\beta)^2 \|e(0)\|^2$. Choosing x_0 as an eigenvector of λ_2 (respectively $\lambda_{\max}$) gives equality. Each factor $E_\beta(-\lambda_i t^\beta)$ is non-increasing in t, so $\|e(t)\|$ is non-increasing.

Step 4 (iv). Insert (2) with $z = \lambda_2 t^\beta$ (upper bound) and $z = \lambda_{\max} t^\beta$ (lower bound) into (12). The lower bound in (13) gives $t^\beta \|e(t)\| \ge \|e(0)\| t^\beta / (1 + \Gamma(1-\beta)\lambda_{\max} t^\beta)$, whose limit as $t \to \infty$ is $\|e(0)\|/(\Gamma(1-\beta)\lambda_{\max}) > 0$. □

Remark 6 (Limiting cases) For $\beta = 1$, (12) is the classical estimate $e^{-\lambda_{\max} t}\|e(0)\| \le \|e(t)\| \le e^{-\lambda_2 t}\|e(0)\|$. As $\beta \to 0^+$, both bounds in (2) tend to $1/(1+z)$, so $E_\beta(-z) \to 1/(1+z)$ and the decay becomes purely hyperbolic. If H^+ is

disconnected, (i)–(ii) still hold and consensus is reached within each component separately; no global consensus occurs. The consensus value is $\bar{x}$ whenever H^+ is connected. It is therefore *independent of the memberships*: memberships affect only the transient, not the limit.

Theorem 12 *Assume H^+ is connected and let $0 < \beta \le 1$, $0 < \varepsilon < 1$.*

(i) (α-cut certificate) $\|e(t)\| \le E_\beta(-\gamma_\alpha(\mu)t^\beta)\|e(0)\|$, with γ_α from (8).

(ii) (Settling time) For any $0 < \gamma \le \lambda_2$ (e.g., $\gamma = \lambda_2$ or $\gamma = \gamma_\alpha$), $\|e(t)\| \le \varepsilon\|e(0)\|$ for all

$$t \;\ge\; T_\varepsilon(\gamma) = \Big(\frac{\Gamma(1+\beta)(\varepsilon^{-1}-1)}{\gamma}\Big)^{1/\beta}.$$

(iii) (Interval certificate) For interval-valued memberships with connected $\operatorname{supp}\mu^L$,

$$\sup_{\mu\in\mathscr{R}}\sup_{e(0)\neq 0}\frac{\|e(t)\|}{\|e(0)\|} = E_\beta\big(-\lambda_2(L_{\mu^L})t^\beta\big),$$

so the pessimistic memberships μ^L certify the decay of every realization, and this certificate cannot be improved.

(iv) (Monotonicity) If $\mu \le \nu$, the worst-case decay curve of ν lies below that of μ for all t and β.

Proof. (i) By Theorem 5, $\gamma_\alpha \le \lambda_2$, and $s \mapsto E_\beta(-st^\beta)$ is non-increasing, so (i) follows from (12). (ii) By (2), $E_\beta(-\gamma t^\beta) \le \varepsilon$ whenever $1 + \gamma t^\beta/\Gamma(1+\beta) \ge \varepsilon^{-1}$, which is $t \ge T_\varepsilon(\gamma)$. (iii) For fixed μ, the inner supremum equals $E_\beta(-\lambda_2(L_\mu)t^\beta)$ by Theorem 11(iii). By Theorem 10, $\min_{\mu\in\mathscr{R}}\lambda_2(L_\mu) = \lambda_2(L_{\mu^L})$, and the function $s \mapsto E_\beta(-st^\beta)$ is decreasing. (iv) follows from Theorem 9 and Lemma 3(a). □

Lemma 6 *Let $f : [0,\infty) \to \mathbb{R}$ be Lipschitz with constant c, and let A, B be symmetric PSD matrices. Then $\|f(A) - f(B)\|_F \le c\,\|A - B\|_F$, where $f(A)$ is defined spectrally.*

Proof. Let $A = \sum_i a_i u_i u_i^\top$ and $B = \sum_j b_j w_j w_j^\top$ be spectral decompositions. Then $u_i^\top(f(A) - f(B))w_j = (f(a_i) - f(b_j))\,u_i^\top w_j$ and $u_i^\top(A - B)w_j = (a_i - b_j)\,u_i^\top w_j$, so $|u_i^\top(f(A) - f(B))w_j| \le c\,|u_i^\top(A - B)w_j|$ for all i, j. Squaring and summing over the orthonormal bases $\{u_i\}$ and $\{w_j\}$ gives the claim. □

Theorem 13 *Let x_μ and x_ν solve (11) with memberships μ, ν and the same x_0, and let $\delta = \mu - \nu$. Then for all $t \ge 0$,*

$$\|x_\mu(t) - x_\nu(t)\| \le \min\Big\{\frac{t^\beta}{\Gamma(1+\beta)}\|L_\mu - L_\nu\|_F,\; E_\beta(-\lambda_2(L_\mu)t^\beta) + E_\beta(-\lambda_2(L_\nu)t^\beta)\Big\}\,\|x_0 - \bar{x}\mathbf{1}\|, \tag{14}$$

with $\|L_\mu - L_\nu\|_F \le \min\{k\sqrt{k-1}\,\|\delta\|_1,\; \sqrt{n-1}\,k\,\ell(\delta)\}$.

Proof. *Step 1.* Let $f_t(s) = E_\beta(-st^\beta)$. By Lemma 3(a), $|f_t'(s)| = t^\beta|g_\beta'(st^\beta)| \le t^\beta/\Gamma(1+\beta)$, so f_t is Lipschitz with this constant. *Step 2.* Since $L\mathbf{1} = 0$ and $f_t(0) = 1$, $f_t(L)\mathbf{1} = \mathbf{1}$ for both Laplacians, so $x_\mu(t) - x_\nu(t) = (f_t(L_\mu) - f_t(L_\nu))(x_0 - \bar{x}\mathbf{1})$. Using $\|\cdot\|_2 \le \|\cdot\|_F$ and Lemma 6 gives the first term. *Step 3.* Writing $x_\mu - x_\nu = (x_\mu - \bar{x}\mathbf{1}) - (x_\nu - \bar{x}\mathbf{1})$ and applying Theorem 11(iii) to each term gives the second term. If $\lambda_2 = 0$, the corresponding factor is 1 and the bound remains valid because $\|f_t(L)(x_0 - \bar{x}\mathbf{1})\| \le \|x_0 - \bar{x}\mathbf{1}\|$. *Step 4.* $\|L_\mu - L_\nu\|_F \le \sum_e |\delta(e)|\,\|L_e\|_F = k\sqrt{k-1}\,\|\delta\|_1$ by Lemma 5. Alternatively, $L_\mu - L_\nu$ has rank at most $n-1$ (it annihilates $\mathbf{1}$), so $\|\cdot\|_F \le \sqrt{n-1}\,\|\cdot\|_2 \le \sqrt{n-1}\,k\,\ell(\delta)$. □

Remark 7 (Interpretation) Theorem 13 shows that membership revisions perturb fractional consensus trajectories at most proportionally to t^β at early times. The effect then fades, because both trajectories converge to the same membership-independent consensus value. The memory exponent β controls both regimes: smaller β gives a slower initial divergence (t^β) but also a slower final convergence ($t^{-\beta}$).

5 Optimal Membership Allocation

A total amount of membership $W \in (0, m]$ is to be distributed over the hyperedges, i.e., $\mu \in \mathscr{P}_W$ (Lemma 2). We consider

$$(\mathrm{P}_{\max}) \quad \rho^*(W) = \max_{\mu\in\mathscr{P}_W}\lambda_{\max}(L_\mu), \qquad\qquad (\mathrm{P}_{\mathrm{gap}}) \quad \gamma^*(W) = \max_{\mu\in\mathscr{P}_W}\lambda_2(L_\mu).$$

By Theorem 11, $(\mathrm{P}_{\mathrm{gap}})$ optimizes the worst-case speed of fractional consensus, while $(\mathrm{P}_{\max})$ maximizes the fastest mode, which governs the initial stiffness of (11) and the lower decay bound. The two objectives have different practical meanings and, as shown below, lead to structurally opposite solutions. Both problems have optimal solutions, since $\mathscr{P}_W$ is compact and the eigenvalues depend continuously on μ.

Theorem 14 *$\mu \mapsto \lambda_{\max}(L_\mu)$ is convex. Hence $(\mathrm{P}_{\max})$ has an optimal solution with at most one fractional membership. For integer W, $\rho^*(W)$ equals the largest spectral radius over crisp sub-hypergraphs with W hyperedges.*

Proof. $\lambda_{\max}(L_\mu) = \max_{\|x\|=1} \sum_e \mu(e) x^\top L_e x$ is a pointwise maximum of linear functions of μ, hence convex. A convex function attains its maximum over a polytope at an extreme point, and the extreme points of $\mathscr{P}_W$ are described in Lemma 2. □

Theorem 15 *$\rho^*(W) \le k \min\{W, \Delta(H)\}$, and $\rho^*(W) = kW$ if and only if $c_2(H) \ge \lceil W \rceil$.*

Proof. *Step 1.* For $\mu \in \mathscr{P}_W$, $d_\mu(v) \le \sum_e \mu(e) = W$, and $d_\mu(v) \le \deg(v)$ because $\mu \le 1$. Theorem 2 then gives the upper bound. *Step 2 ($\Leftarrow$).* Let $u \ne v$ lie in $q \ge \lceil W \rceil$ hyperedges, and spread W over them, which is possible since $\mu \le 1$. For $x = e_u - e_v$, $\mathbf{1}_e^\top x = 0$ and $\|x_e\|^2 = 2$ on these hyperedges, so $x^\top L_\mu x = 2kW = kW\|x\|^2$. *Step 3 ($\Rightarrow$).* If $\lambda_{\max} = kW$, then $d_{\max} = W$ and (5) holds. A vertex with $d_\mu(w) = W = \sum_e \mu(e)$ lies in every hyperedge of E^+, so $V_{\max} \subseteq e$ for all $e \in E^+$. A non-zero x supported on $V_{\max}$ with $\sum_{w \in V_{\max}} x_w = 0$ forces $|V_{\max}| \ge 2$. Any two vertices of $V_{\max}$ then lie in all $|E^+| \ge \lceil W \rceil$ support hyperedges. □

Remark 8 Without the cap $\mu \le 1$, concentrating the whole budget on one hyperedge would give $\lambda_{\max} = kW$ on every hypergraph, and $(\mathrm{P}_{\max})$ would be trivial. The fuzzy cap makes the optimum depend on the higher-order structure through the codegree $c_2(H)$. For graphs ($k = 2$), $c_2 \le 1$, so $\rho^*(W) < 2W$ for all $W > 1$.

Theorem 16 *$\mu \mapsto \lambda_2(L_\mu)$ is concave, so $(\mathrm{P}_{\mathrm{gap}})$ is a convex problem. If the automorphism group of H acts transitively on E, the uniform allocation $\mu \equiv W/m$ is optimal.*

Proof. $\lambda_2(L_\mu) = \min\{\sum_e \mu(e) x^\top L_e x : \|x\| = 1, x \perp \mathbf{1}\}$ is a pointwise minimum of linear functions, hence concave. If μ^* is optimal, so is $\mu^* \circ \sigma$ for every automorphism σ, because $L_{\mu^* \circ \sigma}$ is permutation-similar to L_{μ^*}. By concavity, the average $\bar{\mu} = |\Gamma|^{-1} \sum_\sigma \mu^* \circ \sigma \in \mathscr{P}_W$ is also optimal, and transitivity makes $\bar{\mu}$ constant. □

Corollary 2 *For $K_n^{(k)}$ and $0 < W < \binom{n}{k}$, $\gamma^*(W) = k(k-1)W/(n-1)$ is attained by $\mu \equiv W/\binom{n}{k}$. A crisp allocation attains it if and only if its hyperedges form a 2-(n,k,λ) design, which requires $n(n-1) \mid Wk(k-1)$.*

Proof. $K_n^{(k)}$ is pair-balanced, so the uniform allocation is a fuzzy 2-design and attains (10) by Theorem 6. A crisp allocation attains it iff it is pair-balanced, i.e., a 2-design, whose index $\lambda = Wk(k-1)/(n(n-1))$ must be an integer. □

Corollary 3 *For every $\beta \in (0,1]$ and every $t > 0$, the worst-case disagreement ratio $\sup_{e(0) \ne 0} \|e(t)\|/\|e(0)\| = E_\beta(-\lambda_2(L_\mu) t^\beta)$ is minimized over $\mathscr{P}_W$ exactly by the solutions of $(\mathrm{P}_{\mathrm{gap}})$. No allocation achieves a worst-case ratio below $E_\beta\left(-\frac{k(k-1)W}{n-1} t^\beta\right)$, and on $K_n^{(k)}$ this value is attained by the uniform fuzzy allocation for every budget, but by a crisp allocation only if a 2-design with W blocks exists.*

Proof. Combine Theorem 11(iii), the strict monotonicity in Lemma 3(a), Theorem 6 and Corollary 2. □

Remark 9 (Uniform versus concentrated memberships) Theorems 14 and 16 identify a dichotomy. Spectral concentration $(\mathrm{P}_{\max})$ is always achieved by crisp, all-or-nothing allocations. Robust and fast fractional consensus $(\mathrm{P}_{\mathrm{gap}})$ generally requires graded memberships that fill the gaps left by crisp sub-hypergraphs. This optimality holds for every memory order β simultaneously.

6 The SPEC-FC Algorithm and Computational Complexity Analysis

This section turns the theory into a computational procedure (Algorithm 1). The procedure takes raw observations of a higher-order system, builds the fuzzy-weighted hypergraph, and returns spectral diagnostics, stability certificates, fractional consensus certificates and optimal membership allocations.

Algorithm 1 SPEC-FC: spectral and fractional-consensus analysis of a fuzzy-weighted uniform hypergraph

Require: vertex set V ($|V| = n$), uniformity k, observations defining candidate hyperedges, fractional orders $\{\beta\}$, tolerance ε, budget W (optional)

Ensure: spectrum of L_μ, α-cut certificates, stability bounds, settling times, optimal allocations

Phase 1: Construction
Step 1: Determine the hyperedge set E ($|E| = m$) and the membership $\mu(e) \in [0,1]$ of every $e \in E$
Step 2 (optional): Determine interval memberships $[\mu^L(e), \mu^U(e)]$
Phase 2: Spectral analysis
Step 3: Assemble $L_\mu = \sum_e \mu(e)(kI_e - \mathbf{1}_e\mathbf{1}_e^\top)$
Step 4: Compute the spectrum and check connectivity of H^+ (Theorem 1)
Step 5: Compute the radius bounds (Theorem 2) and the budget bound (Theorem 6)
Step 6: For each distinct membership level α_j, compute $\lambda_2(L(H_{\alpha_j}))$ and $\lambda_{\max}(L(H_{\alpha_j}))$; form γ_α and the bound (9)
Phase 3: Stability
Step 7: For a revision ν, compute $\ell(\mu - \nu)$, the localized bound and the one-sided gap certificate (Theorems 7, 8)
Step 8: Compute $\lambda_i(L_{\mu^L})$, $\lambda_i(L_{\mu^U})$ (Theorem 10)
Phase 4: Fractional consensus
Step 9: For each β, evaluate $E_\beta(-\lambda t^\beta)$ at $\lambda \in \{\lambda_2, \gamma_\alpha, \lambda_2(L_{\mu^L})\}$ and the settling times T_ε (Theorems 11, 12)
Phase 5: Optimization (if W is given)
Step 10: Solve $(\mathrm{P}_{\mathrm{gap}})$ by projected super-gradient ascent: $\mu \leftarrow \Pi_W\big(\mu + \eta_0 t^{-1/2} g/\|g\|\big)$, $g(e) = k\|x_e\|^2 - (\mathbf{1}_e^\top x)^2$, x a unit eigenvector of λ_2
Step 11: If $c_2(H) \geq \lceil W \rceil$, return the certified optimum kW (Theorem 15); otherwise search extreme points of $\mathscr{P}_W$ exhaustively when $\binom{m}{\lfloor W \rfloor}$ is small (Theorem 14), or run projected gradient ascent from several random starts (local search, no optimality guarantee)
Phase 6: Sensitivity
Step 12: Repeat Steps 4–11 under variations of β, μ, k and W

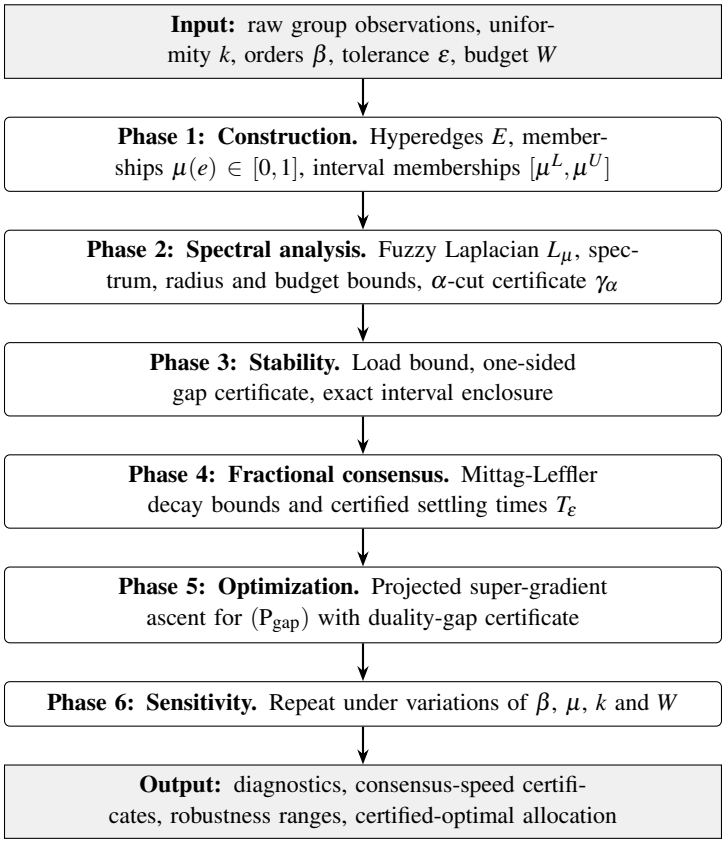


Figure 1 Flowchart of the proposed SPEC-FC decision-support procedure (Algorithm 1).

Here $\Pi_W(y) = \min\{\max\{y - \tau\mathbf{1}, 0\}, \mathbf{1}\}$ is the Euclidean projection onto $\mathscr{P}_W$. The scalar τ is found by bisection, because $\tau \mapsto \sum_e \min\{\max\{y_e - \tau, 0\}, 1\}$ is non-increasing. Since $(\mathrm{P}_{\mathrm{gap}})$ is concave (Theorem 16), the standard analysis of super-

gradient ascent with normalized steps $\eta_t = \eta_0 t^{-1/2}$ gives $\gamma^* - \max_{t\le T} \lambda_2(L_{\mu^{(t)}}) \le G(R^2+\eta_0^2(1+\ln T))/(2\eta_0 \sum_{t\le T} t^{-1/2}) = O(\ln T/\sqrt{T})$, where $R = \operatorname{diam} \mathscr{P}_W$ and G bounds the super-gradient norms; this assumes exact eigenvectors and an exact projection (our bisection tolerance is 10^{-12}). Independently of this rate, every iterate yields a computable optimality certificate: for any $Y \succeq 0$ with $\operatorname{tr} Y = 1$ and $Y\mathbf{1} = 0$, weak duality gives $\gamma^* \le \max_{\mu\in\mathscr{P}_W} \operatorname{tr}(YL_\mu)$, which equals the sum of the $\lfloor W \rfloor$ largest values $\operatorname{tr}(YL_e)$ plus $(W - \lfloor W \rfloor)$ times the next one. We take Y as the normalized projector onto the eigenvectors whose eigenvalues are close to λ_2 at the best iterate. The Mittag-Leffler function is evaluated by its power series for $z \le 0.5$ and by its Laplace-type integral representation otherwise (adaptive quadrature with absolute tolerance 10^{-16} and relative tolerance 10^{-13}); see [28] for reliable alternatives.

6.1 Computational Complexity

All scalar operations are counted as $O(1)$. Let $r \le m$ be the number of distinct membership levels, N_β the number of fractional orders, N_t the number of time points, and q the cost of one Mittag-Leffler evaluation, which is independent of n, m, k.

1. *Step 3 (assembly).* Each hyperedge updates a $k \times k$ block: $O(mk^2)$.
2. *Step 4 (spectrum).* Dense symmetric eigen-decomposition: $O(n^3)$. Connectivity of H^+ by union–find: $O(mk)$.
3. *Step 5.* Fuzzy degrees and codegrees: $O(mk^2)$.
4. *Step 6.* One assembly and one eigen-decomposition per level: $O(r(n^3 + mk^2))$.
5. *Step 7.* The load costs $O(mk)$. The Loewner bound needs one further eigen-decomposition, $O(n^3 + mk^2)$.
6. *Step 8.* Two eigen-decompositions: $O(n^3 + mk^2)$.
7. *Step 9.* $O(N_\beta N_t q)$ for the certificates. Trajectories via (3) cost an additional $O(N_\beta N_t(n^2 + nq))$.
8. *Step 10.* Per iteration: assembly $O(mk^2)$, eigen-decomposition $O(n^3)$, super-gradient $O(mk)$, projection $O(m\log(1/\varepsilon))$; over T iterations, $O(T(n^3 + mk^2 + m\log(1/\varepsilon)))$.
9. *Step 11.* The codegree test costs $O(mk^2)$. Exhaustive extreme-point search costs $\binom{m}{W}$ eigen-decompositions for integer W, and $\binom{m}{\lfloor W \rfloor}(m - \lfloor W \rfloor)$ otherwise; it is feasible only for small m. Local search costs $O(n^3 + mk^2 + m\log(1/\varepsilon))$ per iteration and has no optimality guarantee.

Table 4 Computational complexity of the phases of Algorithm 1.

Phase	Cost	Dominant term
Construction and assembly	$O(mk^2)$	mk^2
Spectral analysis	$O(n^3 + mk^2)$	n^3
α-cut certificates	$O(r(n^3 + mk^2))$	rn^3
Stability and interval enclosure	$O(n^3 + mk^2)$	n^3
Fractional certificates	$O(N_\beta N_t q)$	$N_\beta N_t$
$(\mathrm{P}_{\mathrm{gap}})$, T iterations	$O(T(n^3 + mk^2 + m\log(1/\varepsilon)))$	Tn^3
$(\mathrm{P}_{\max})$, exhaustive	$O\big(\binom{m}{\lfloor W \rfloor} m(n^3 + mk^2)\big)$	combinatorial
$(\mathrm{P}_{\max})$, local search	$O(T(n^3 + mk^2 + m\log(1/\varepsilon)))$	Tn^3

Apart from the exhaustive search in $(\mathrm{P}_{\max})$, which is used only for validation, every step is polynomial. The cubic dependence on n comes from dense eigen-decompositions. For large sparse hypergraphs it can be replaced by Lanczos iterations for λ_2 and $\lambda_{\max}$, at cost $O(\min\{n^2, n + mk^2\})$ per iteration.

7 Case Study 1: Cohesion Analysis of the Davis Southern Women Affiliation Data

7.1 Motivation and Choice of Application

We sought real data that (a) contain genuinely higher-order interactions, (b) admit a uniform representation without arbitrary choices, (c) yield membership degrees with a transparent meaning, and (d) are publicly available and citable. Several candidate domains were considered. Supply-chain, transportation, infrastructure and biological interaction data are usually proprietary or available only as pairwise links, and memberships would have to be invented. Communication and

contact records are higher-order but larger; Section 8 shows that the same construction applies to sensor-recorded group contacts. For a first, fully transparent illustration, the Davis Southern Women affiliation data satisfy all four requirements. They were collected in an ethnographic field study and published by Davis, Gardner and Gardner (*Deep South*, University of Chicago Press, 1941). They record which of 18 women attended which of 14 social events, and they are among the most frequently re-analysed social-network datasets. We use the version distributed with the open-source Python library NetworkX (version 3.7, function `davis_southern_women_graph`). Their structure is intrinsically higher-order: an event is a group, not a set of pairs.

7.2 Dataset

The data comprise $n = 18$ women, 14 events and 89 recorded attendances. Event sizes range from 3 to 14 (events E1–E14 have sizes $3,3,6,4,8,8,10,14,12,5,4,6,3,3$). No value is missing, and no woman or event is excluded. Let $A_i \subseteq \{1,\dots,14\}$ denote the set of events attended by woman i.

7.3 Construction of the Fuzzy-Weighted Uniform Hypergraph

The events themselves form a non-uniform hypergraph. Rather than treating it as uniform, which would be invalid, we use the smallest genuinely higher-order unit, the *triad*, and set $k = 3$:

$$V = \{1,\dots,18\}, \quad E = \Big\{\{u,v,w\} : A_u \cap A_v \cap A_w \neq \emptyset\Big\}, \quad \mu(\{u,v,w\}) = \frac{|A_u \cap A_v \cap A_w|}{|A_u \cup A_v \cup A_w|}. \tag{15}$$

A triad is a hyperedge if its three members attended at least one event together. Each event of size s thus generates its $\binom{s}{3}$ triads. This gives $m = 586$ of the $\binom{18}{3} = 816$ possible triads. The construction is deterministic, and the choice $k = 3$ is examined in Section 11.

7.4 Membership Specification

The membership (15) is the generalized Jaccard ratio of the three attendance sets. It equals the fraction of the triad's observed social activity that is shared by all three members, and it is the degree to which the triad belongs to the fuzzy concept "cohesive triad". It equals 1 iff the three women attended exactly the same events, and it is positive iff they co-attended at least once. It is *not* a probability, since no sampling model is assumed. Nor is it an unbounded importance weight: the raw count $|A_u \cap A_v \cap A_w|$ (at most 5 here) is such a weight and is used as a baseline in Section 9. Measurement uncertainty is modelled separately by interval-valued memberships. Let $\mu^{(-j)}$ be (15) recomputed after deleting event j from the record. Then

$$\mu^L(e) = \min\{\mu(e), \mu^{(-1)}(e), \dots, \mu^{(-14)}(e)\}, \qquad \mu^U(e) = \max\{\mu(e), \mu^{(-1)}(e), \dots, \mu^{(-14)}(e)\} \tag{16}$$

quantifies how much each membership depends on any single observed event.

Table 5 shows the distribution of μ. Memberships lie in $[0.071, 0.571]$, with median 0.125, quartiles 0.100 and 0.217, and total $W = 97.692$. No triad is fully cohesive. The interval half-widths average 0.063, and 365 triads have $\mu^L = 0$ because they share a single event.

Table 5 Distribution of the 586 triad memberships $\mu(e)$ in the Davis data.

$[0.0,0.1)$	$[0.1,0.2)$	$[0.2,0.3)$	$[0.3,0.4)$	$[0.4,0.5)$	$[0.5,0.6)$	$[0.6,0.7)$	$[0.7,0.8)$	$[0.8,0.9)$	$[0.9,1.0]$
133	275	115	37	18	8	0	0	0	0

7.5 Experiment A: Baseline Spectral Analysis

The fuzzy Laplacian has $\lambda_2(L_\mu) = 13.2545$ and $\lambda_{\max}(L_\mu) = 49.5017$. The support hypergraph is connected (Theorem 1). The largest fuzzy degree is $d_{\max} = 22.792$ (Ruth DeSand), so Theorem 2 gives $45.584 < 49.502 \leq 68.376$. The α-cut bound (9), 53.364, is sharper. Theorem 6 gives $\lambda_2 \leq 34.480 \leq \lambda_{\max}$. The ratio $\lambda_2/34.480 = 0.38$ measures how far the observed cohesion structure is from a fuzzy 2-design, i.e., from an equal distribution of shared activity over all pairs.

Table 6 lists the women with the largest fuzzy degrees. Fuzzy degree is not the same as activity: Ruth DeSand and Verne Sanderson attended only four events each, yet they rank first and third. Their few events were the large central ones (E7–E9), which generate many triads with substantial shared activity.

The eigenvector of λ_2 (Fiedler vector) splits the women into two groups of nine. Group I contains Evelyn, Laura, Theresa, Brenda, Charlotte, Frances, Eleanor, Ruth and Helen. Group II contains Pearl, Verne, Myra, Katherina, Sylvia,

Table 6 The five largest fuzzy degrees (Davis data).

Woman	Events attended	Triads containing her	$d_\mu(v)$	$(L_\mu)_{vv} = 2d_\mu(v)$
Ruth DeSand	4	119	22.792	45.584
Theresa Anderson	8	120	22.389	44.777
Verne Sanderson	4	117	21.528	43.055
Pearl Oglethorpe	3	109	19.221	38.442
Sylvia Avondale	7	117	18.979	37.958

Nora, Dorothy, Olivia and Flora. We report this partition as an output of the model, without claiming agreement with any particular ethnographic grouping.

7.6 Experiment B: α-Cut Analysis

The memberships take $r = 23$ distinct values. The resolution (7) was verified numerically with maximal entrywise error 4.3×10^{-14}. Table 7 shows how the crisp structure degrades as the confidence threshold α increases. The cut hypergraph remains connected up to $\alpha^* = 1/3$ (63 triads, $\lambda_2(L(H_{\alpha^*})) = 0.961$), splits into five components at $\alpha = 0.4$, and has no hyperedge for $\alpha \geq 0.6$.

Table 7 Crisp α-cut hypergraphs of the Davis data. Comp.: connected components; Iso.: isolated vertices.

α	$\lvert E_\alpha \rvert$	Comp.	Iso.	$\lambda_2(L(H_\alpha))$	$\alpha\,\lambda_2(L(H_\alpha))$	$\lambda_{\max}(L(H_\alpha))$
0.05	586	1	0	92.1849	4.6092	255.5325
0.10	453	1	0	62.8377	6.2838	238.4495
0.15	252	1	0	24.5044	3.6757	156.7494
0.20	178	1	0	13.9045	2.7809	121.6968
0.25	114	1	0	4.8730	1.2182	77.0261
0.30	63	1	0	0.9606	0.2882	44.1416
0.40	26	5	3	-0.0000	-0.0000	24.4273
0.50	8	10	8	0.0000	0.0000	14.0000
0.60	0	18	18	0.0000	0.0000	0.0000
0.80	0	18	18	0.0000	0.0000	0.0000
1.00	0	18	18	0.0000	0.0000	0.0000

These numbers illustrate the practical value of Theorem 5. No single crisp threshold represents the data well. Low thresholds treat incidental co-attendance as full membership, and high thresholds disconnect the structure. The best single-level bound in (8) is only $\max_j \alpha_j \lambda_2(L(H_{\alpha_j})) = 6.920$, attained at $\alpha = 1/12$; the minimum-membership bound (the level $\alpha_1 = 1/14$) is 6.585. In contrast, the level-averaged bound $\gamma_\alpha = 11.747$ recovers 89% of the true value 13.255 by combining all thresholds.

7.7 Experiment C: Spectral Stability under Real and Synthetic Perturbations

C1: deleting one event. Removing event j from the record is a real revision of the memberships. It is *not* localized: the Jaccard denominator changes for every triad containing an attendee of j, so between 268 and 585 of the 586 memberships change (column "Changed"). These revisions therefore test the bounds of Theorem 7 for revisions of widely varying extent; genuinely localized revisions are studied in C2. Table 8 compares the observed largest eigenvalue shift with the bounds of Theorem 7, and the post-deletion λ_2 with the one-sided certificate of Theorem 8.

All bounds hold. On average, the Weyl bound overestimates the observed shift by a factor of 6.8 and the load bound by 2.5; the Weyl bound exceeds the load bound by a factor of 2.7 (at most 4.0). More importantly, the one-sided certificate guarantees $\lambda_2 > 0$, i.e., that the cohesion structure survives the loss of the event, for 12 of the 14 deletions. The Weyl-based certificate $\lambda_2 - 3\|\delta\|_1$ gives no guarantee for any deletion. The two failures are the largest events, E8 and E9. Deleting E9 lowers λ_2 from 13.25 to 0.65, and it identifies this event as structurally critical for the cohesion of the group.

C2: localized versus global noise. We perturbed either all triads containing one randomly chosen woman (localized) or all triads (global) by $\pm\varepsilon$, with 200 trials each (Table 9). For localized noise the load and Weyl bounds coincide, as predicted by Theorem 7: all revisions touch the same vertex, so $\ell(\delta) = \|\delta\|_1$. For global noise the Weyl bound is about 4.9 times larger than the load bound.

C3: interval-valued memberships. Table 10 reports the exact enclosure of Theorem 10 for the leave-one-event-out intervals (16), together with the range over 2000 uniformly sampled realizations (maximal violation 5.3×10^{-14}). The

Table 8 Effect of deleting a single event. Changed: triads whose membership changes. Cert.: one-sided certificate $\lambda_2(L_\mu) - 3\,\ell((\mu-\nu)_+)$ (Theorem 8).

Event	Size	Changed	Observed shift	$\lambda_{\max}(L_{\lvert\delta\rvert})$	$3\,\ell(\delta)$	Weyl $3\lVert\delta\rVert_1$	New λ_2	Cert.
E1	3	270	3.261	4.629	6.282	14.940	13.692	13.088
E2	3	290	4.258	5.471	7.632	16.123	13.819	13.088
E3	6	404	3.409	5.887	8.180	23.734	13.508	10.445
E4	4	314	3.868	5.602	7.799	17.723	13.846	12.546
E5	8	480	3.552	10.038	14.029	36.523	11.756	6.558
E6	8	508	4.655	9.661	13.448	39.133	14.273	7.161
E7	10	541	4.129	12.655	17.206	58.890	9.279	2.819
E8	14	585	15.801	22.089	30.671	121.945	9.074	-14.739
E9	12	567	16.028	17.827	24.304	92.831	0.651	-8.709
E10	5	404	3.223	6.286	8.675	22.220	14.095	11.618
E11	4	268	2.602	4.419	6.173	15.784	14.225	12.088
E12	6	456	3.833	8.012	11.091	28.005	14.328	10.283
E13	3	284	3.112	4.909	6.769	13.787	13.818	13.088
E14	3	284	3.112	4.909	6.769	13.787	13.818	13.088

Table 9 Mean eigenvalue shift and bounds under $\pm\varepsilon$ noise (200 trials each).

Noise	ε	Observed shift	Load $3\,\ell(\delta)$	Weyl $3\lVert\delta\rVert_1$	Weyl/load
localized	0.02	0.2879	5.9322	5.9322	1.0
localized	0.05	0.6717	14.7945	14.7945	1.0
localized	0.10	1.3267	28.4052	28.4052	1.0
global	0.02	0.6073	7.2000	35.1600	4.9
global	0.05	1.5165	18.0000	87.9000	4.9
global	0.10	2.8929	35.4971	172.1259	4.8

exact range of λ_2 is $[0.154, 15.269]$. Sampling finds only $[6.600, 9.434]$, because uniform realizations concentrate near the centre of the 586-dimensional box. The pessimistic memberships μ^L still have a connected support, so by Corollary 1 and Theorem 10 *every* realization is connected. This robustness statement could not be obtained by sampling.

The box $[\mu^L, \mu^U]$ must be interpreted with care. It is a *conservative outer enclosure* of the leave-one-event-out sensitivity, not a statistical confidence region. It treats the 586 memberships as varying independently, whereas the deletion of one event moves them jointly, and it considers only deletions, not possibly unrecorded attendances. Over the 15 actual scenarios (full data and the 14 single deletions), λ_2 ranges only over $[0.651, 14.328]$, compared with $[0.154, 15.269]$ for the box. Certificates derived from μ^L are therefore valid but pessimistic.

Table 10 Exact eigenvalue enclosure of the conservative leave-one-event-out box $[\mu^L, \mu^U]$.

Eigenvalue	$\lambda_i(L_{\mu^L})$	Sampled min	Nominal $\lambda_i(L_\mu)$	Sampled max	$\lambda_i(L_{\mu^U})$
λ_2	0.154	6.600	13.255	9.434	15.269
λ_3	0.429	7.944	17.307	12.785	19.806
λ_4	4.961	11.179	17.574	14.200	20.980
λ_{17}	20.915	35.592	47.934	40.708	53.930
λ_{18}	26.450	38.219	49.502	42.618	56.595

7.8 Experiment D: Illustrative Fractional Dynamics on an Empirical Interaction Structure

This experiment is a mathematical illustration, not an empirical study of social dynamics: no opinions or time-resolved behaviour were observed, and the fractional order β, the time scale (coupling constant 1) and the initial state are assumptions. We run (11) on the empirically constructed hypergraph with the initial state $x_0(v) = |A_v|/14$ (participation rate), used only as a heterogeneous test vector. Settling times are therefore in arbitrary time units. Table 11 reports the time after which the worst-case disagreement ratio is at most $\varepsilon = 0.1$. It is computed exactly from $E_\beta(-\lambda_2 t^\beta)$ (Theorem 11), and certified from the α-cut bound γ_α, the minimum-membership bound and the interval-robust value $\lambda_2(L_{\mu^L})$ (Theorem 12).

Table 11 Times t with $E_\beta(-\lambda t^\beta) = 0.1$ for different spectral inputs λ (Davis data).

β	Exact ($\lambda_2 = 13.255$)	α-cut ($\gamma_\alpha = 11.747$)	Min-membership (6.585)	Interval-robust (0.154)
0.4	0.158	0.214	0.909	10790.425
0.6	0.182	0.222	0.583	303.162
0.8	0.175	0.204	0.420	45.712
1.0	0.174	0.196	0.350	14.908

The α-cut certificate is within 13–35% of the exact settling time for all β, while the minimum-membership certificate overestimates it by a factor of 2–6. The interval-robust certificate illustrates the effect of memory: for the conservative box of Experiment C3, the guaranteed settling time grows from 14.9 ($\beta = 1$) to 10790 ($\beta = 0.4$), reflecting the algebraic tail $t^{-\beta}$ of Theorem 11(iv). These values are driven by the pessimism of the box and should not be read as properties of the data.

7.9 Experiment E: Budget-Constrained Membership Allocation

The budget W is interpreted abstractly as a limited cohesion capacity distributed over the existing triads ($\mu \le 1, \sum \mu = W$). The optimized memberships are a design target and are not, in general, the Jaccard memberships of any attendance matrix. Table 12 compares four quantities:

- the observed memberships rescaled to total W;
- the best of 5000 random crisp allocations with $\lfloor W \rfloor$ hyperedges of membership 1 and one hyperedge of membership $W - \lfloor W \rfloor$ (an extreme point of $\mathscr{P}_W$, Lemma 2); this is a heuristic baseline, not the crisp optimum;
- the numerically optimized value of $(\mathrm{P}_{\mathrm{gap}})$ (Algorithm 1, six starts, 3000 iterations);
- its weak-duality upper bound (Section 6).

For $(\mathrm{P}_{\max})$, the table reports the best value found by local search, which is certified optimal only when it attains $3W$ (Theorem 15).

Table 12 Budget-constrained allocation on the Davis hypergraph ($c_2(H) = 16$, $\Delta(H) = 120$). Frac.: number of strictly fractional optimized memberships.

W	Observed (rescaled) λ_2	Random crisp (best of 5000)	Optimized fuzzy λ_2	Dual upper bound	Bound (10)	Frac.	Best $\lambda_{\max}$ found	$3\min\{W,\Delta\}$
10.00	1.3568	0.5293	3.0769	3.0769	3.5294	405	30.000	30.0
20.00	2.7135	2.6028	6.1538	6.1538	7.0588	388	52.805	60.0
97.69	13.2545	19.8412	29.4447	29.4447	34.4796	422	207.934	293.1

The optimized values are certified: the duality gap is 4×10^{-10}, 1×10^{-9} and 2.7×10^{-5} for $W = 10$, 20 and 97.69. At the observed budget, the optimal allocation raises λ_2 from 13.25 to 29.44 (factor 2.22), within 15% of the universal bound 34.48; no fuzzy 2-design exists in $\mathscr{P}_W$ for this hypergraph, so that bound is not attained. The best random crisp allocation reaches 19.84. Since settling times scale exactly as $\lambda_2^{-1/\beta}$, the optimal allocation shortens them by a factor $2.22^{1/\beta}$, i.e., 2.22 for $\beta = 1$, 3.13 for $\beta = 0.7$ (from 0.180 to 0.058) and 4.94 for $\beta = 0.5$. Structurally, the optimum moves membership away from already strong triads: the share of W on triads with above-median membership falls from 74% to 41%, and the coefficient of variation of the fuzzy degrees falls from 0.28 to 0.08.

The radius objective behaves differently, in accordance with Theorems 14 and 15. For $W = 10 \leq c_2 = 16$, the value $\lambda_{\max} = 30 = 3W$ is certified optimal and is attained by concentrating membership on ten triads that share a common pair of women. For $W = 20$ and $W = 97.69$ the reported values come from local search and are not certified; the upper bounds are 60 and 293.1. Maximizing $\lambda_{\max}$ creates a tight core that accelerates only the fastest mode. It does *not* improve consensus as a whole, so the two objectives must not be conflated.

7.10 Practical Interpretation and Limitations

For this dataset, the fuzzy model contributes the following information that the crisp models do not provide (see also Section 9).

- A balanced two-group Fiedler split that is not driven by activity levels.
- A level-averaged connectivity certificate that no single threshold can deliver.
- A guarantee that the cohesion structure survives the loss of any of 12 of the 14 events, together with the identification of the two critical events.
- Exact robustness ranges under data incompleteness.
- A certified-optimal membership allocation that raises λ_2 by a factor 2.22, shortening settling times by $2.22^{1/\beta}$.

Some findings, such as the Fiedler partition itself, follow from standard spectral graph theory applied to the weighted clique expansion. The α-cut, one-sided, interval and capped-budget results are specific to the fuzzy framework.

The application also has limitations. The data are historical and small; a larger, recent dataset is analysed in Section 8. The triadic construction is a modelling choice (examined for $k = 2,4$ in Section 11). The initial state of the consensus model is a proxy rather than a measured opinion. The budget experiment is a design exercise, not an intervention that was carried out. The membership definition (15) weights all events equally, so large events (E8 alone generates $\binom{14}{3} = 364$ triads) dominate the triad set; size-discounted memberships are a natural alternative. The results therefore illustrate the framework on real data, but they are not an empirical validation of the fractional dynamics.

8 Case Study 2: Face-to-Face Group Contacts in a High School

The Davis data are small and historical. To test the framework on a larger and recent system, and on interactions recorded by sensors rather than by an observer, we use the face-to-face contacts among the students of a high school in Marseilles, France, collected with wearable proximity sensors during one week in December 2013 [11]. We use the timestamped-simplex version of the data [40]. In this version, for every 20-second interval, every maximal clique of simultaneous contacts forms one simplex. The data contain 172,035 timestamped simplices on 327 students over five school days.

8.1 Construction

Most simplices are pairs. We call a simplex with at least three students a *group contact*; there are 8058 of them (7475 of size 3, 576 of size 4 and 7 of size 5). Let A_i be the set of group contacts in which student i takes part. As for the Davis data, we set $k = 3$, let E be the triads that are contained in at least one group contact, and define the membership by the

generalized Jaccard ratio

$$\mu(\{u,v,w\}) = \frac{|A_u \cap A_v \cap A_w|}{|A_u \cup A_v \cup A_w|}.$$

The support hypergraph is connected and covers 317 students; the remaining 10 students never take part in a group contact. The result is a fuzzy 3-uniform hypergraph with $n = 317$ vertices, $m = 2370$ hyperedges and total membership $W = 40.355$. Memberships range from 0.0011 to 0.683 with median 0.0063; 1552 triads have $\mu < 0.01$ and only 20 have $\mu \geq 0.2$. The memberships are small because each student takes part in many group contacts and most triads meet only a few times. Recording days are separated by the overnight gaps in the timestamps. Deleting one day from the record is the real revision studied in Experiment C1 below, and the five deletions define interval-valued memberships $\mu^L = \min\{\mu, \mu^{(-1)}, \ldots, \mu^{(-5)}\}$ and $\mu^U = \max\{\mu, \mu^{(-1)}, \ldots, \mu^{(-5)}\}$, as in (16).

8.2 Spectral Diagnostics and α-Cuts

The fuzzy Laplacian has $\lambda_2 = 0.00958$ and $\lambda_{\max} = 2.664$. Since $d_{\max} = 1.037$, Theorem 2 gives $2.075 < \lambda_{\max} \leq 3.112$, and the budget bound of Theorem 6 gives $\lambda_2 \leq 6W/316 = 0.766$. The small value of λ_2 reflects the class structure of the school: students meet mostly within their classes.

Table 13 shows that thresholding destroys the structure quickly. The α-cut hypergraph is connected only for $\alpha \leq \alpha^* = 0.0032$. Already at $\alpha = 0.005$ it has two components, and at $\alpha = 0.05$ it has 127 components and 95 isolated students. A crisp model built from any reasonable threshold therefore predicts that consensus is impossible, whereas the fuzzy model retains a connected structure. The α-cut certificate of Theorem 5 gives $\lambda_2 \geq 0.00378$, that is, 39.5% of the exact value. The minimum-membership bound gives only 0.00141 (14.8%), so the α-cut certificate is 2.68 times stronger.

Table 13 α-cut hypergraphs of the high-school contact data ($n = 317$, $m = 2370$). Iso.: students covered by no hyperedge of the cut.

α	Hyperedges	Components	Iso.	$\lambda_2(H_\alpha)$	$\lambda_{\max}(H_\alpha)$
0.002	2264	1	0	1.2274	164.039
0.005	1431	2	1	0.0000	77.766
0.010	818	7	6	0.0000	55.816
0.020	442	19	17	0.0000	36.741
0.050	149	127	95	0.0000	15.535
0.100	65	217	180	0.0000	10.518
0.200	20	284	271	0.0000	8.000

8.3 Robustness to the Loss of a Recording Day

Table 14 reports the effect of deleting one recording day. Each deletion changes almost all memberships (2348 to 2368 of 2370). The load bound of Theorem 7 holds in every case. On average it overestimates the observed eigenvalue shift by a factor of 15.5, whereas the Weyl bound $3\|\delta\|_1$ overestimates it by a factor of 279; the load bound is thus 18 times sharper. Unlike in the Davis data, no single day is dispensable here: every deletion disconnects the triadic structure (into 2 to 10 components), so λ_2 drops to 0. The one-sided certificate of Theorem 8 is negative in all five cases, so it gives no false guarantee.

Table 14 Effect of deleting one recording day from the high-school data. Events: group contacts on that day. Changed: triads whose membership changes. Load: $3\ell(\delta)$ (Theorem 7). Weyl: $3\|\delta\|_1$. Cert.: one-sided certificate $\lambda_2(L_\mu) - 3\ell((\mu - \nu)_+)$ (Theorem 8).

Deleted	Events	Changed	Observed shift	Load	Weyl	New λ_2	Cert.
Day 1	1625	2355	0.0993	1.6898	39.562	0.00000	-1.65768
Day 2	1906	2368	0.1408	1.9599	45.779	0.00000	-1.51481
Day 3	1754	2360	0.2478	3.7112	49.021	0.00000	-2.66429
Day 4	1527	2348	0.1609	2.3714	37.757	0.00000	-2.03920
Day 5	1246	2350	0.1077	1.8176	25.702	0.00000	-1.15536

The interval-valued memberships make the same point quantitatively. For 2060 of the 2370 triads the lower membership is 0, because those triads met on a single day, and the support of μ^L has 115 components. Theorem 10 therefore gives the exact enclosure $\lambda_2 \in [0, 0.0161]$ over the whole box. Five hundred random memberships drawn from the box gave $\lambda_2 \in$

$[4.6 \times 10^{-6}, 0.0087]$, with no violation of the enclosure (largest violation 3.2×10^{-15}). The robust fractional certificate is therefore infinite. This is not a weakness of the bound: the enclosure is exact, and it shows that one week of contacts does not support a guarantee of group cohesion that survives the loss of a day.

8.4 Fractional Settling-Time Certificates

Table 15 gives the time needed for the disagreement to fall below 10% of its initial value, $\varepsilon = 0.1$, for several fractional orders. Because settling times scale as $\gamma^{-1/\beta}$ for a certified rate γ, the gap between a certificate and the exact value widens as the memory becomes stronger. The α-cut certificate exceeds the exact settling time by a factor of 2.5 for $\beta = 1$ and 10.2 for $\beta = 0.4$, whereas the minimum-membership certificate exceeds it by factors of 6.8 and 120. Its relative tightness is lower than on the Davis data, because the memberships here are spread over more than a thousand distinct levels and are concentrated near zero.

Table 15 Settling times ($\varepsilon = 0.1$) on the high-school data: exact value, α-cut certificate, minimum-membership certificate and interval-robust certificate (Theorem 12).

β	Exact	α-cut certificate	Min-membership certificate	Interval-robust
0.4	1.126e+07	1.148e+08	1.347e+09	∞
0.6	3.119e+04	1.467e+05	7.573e+05	∞
0.8	1477	4716	1.615e+04	∞
1.0	240.3	608.4	1629	∞

8.5 Budget-Constrained Membership Allocation

At the observed budget $W = 40.355$, Algorithm 1 raises λ_2 from 0.00958 to 0.11821, a factor of 12.3. Four starts (the observed memberships, the uniform allocation and two random allocations) reached 0.1178–0.1179 after 3000 iterations, and continuing the best start for 12,000 iterations gives 0.11821. To certify the result at this size, the weak-duality bound of Section 6 was sharpened by optimizing the test matrix within the span of the s eigenvectors of smallest non-zero eigenvalue, $Y = V_S Z V_S^\top$ with $Z \succeq 0$ and $\operatorname{tr} Z = 1$. Every feasible Z gives a valid upper bound, and this is a small semidefinite program. With $s = 40$ it gives $\gamma^* \leq 0.11896$. The computed allocation is therefore within 0.64% of the optimum.

The comparison with crisp allocations is decisive here. A crisp allocation with budget W has at most $\lfloor W \rfloor + 1 = 41$ hyperedges of positive membership, whereas a connected 3-uniform hypergraph on 317 vertices needs at least $\lceil 316/2 \rceil = 158$ hyperedges. Hence $\lambda_2 = 0$ for every crisp allocation and for every extreme point of $\mathscr{P}_W$. Only graded memberships can make consensus possible at this budget, in line with Theorem 16. The optimal allocation has 625 strictly fractional memberships, sets 1745 to zero and none to one. It moves membership away from the strongest triads: their share of W (triads with above-median membership) falls from 88.9% to 44.0%. Since settling times scale as $\lambda_2^{-1/\beta}$, the optimal allocation shortens them by the factor $12.34^{1/\beta}$, that is, 12.3 for $\beta = 1$, 36.2 for $\beta = 0.7$ and 535 for $\beta = 0.4$.

8.6 Summary of the Second Application

On a recent sensor-recorded system with more than 17 times as many actors as the Davis data, the framework (i) shows that the fuzzy model keeps a connected structure that every non-trivial crisp threshold destroys; (ii) yields an α-cut certificate 2.7 times stronger than the minimum-membership bound; (iii) provides perturbation bounds 18 times sharper than Weyl's for real revisions of the record; (iv) gives an exact, and in this case negative, robustness verdict; and (v) finds an allocation, certified within 0.64% of optimal, that no crisp allocation can approach. The memberships describe co-presence, not opinions, and the allocation is a design target rather than an intervention, so these results illustrate the framework and are not an empirical validation of the fractional dynamics.

9 Comparative Analysis of the FFHC Framework and Existing Models

The comparison has two parts. First, the proposed model is compared with alternative representations of the same real data. Second, the proposed bounds and certificates are compared with the classical ones on a large set of random instances. The purpose is to identify mathematical differences, not to claim universal superiority.

9.1 Comparison of Models on the Davis Data

Seven Laplacians were built from the same attendance records:

- (M1) the unweighted 3-uniform hypergraph (support of μ);
- (M2) the crisp α-cut at the largest connected threshold $\alpha^* = 1/3$;
- (M3) the crisp α-cut at $\alpha = 0.5$;
- (M4) the conventional weighted clique expansion of the events, with pair weights equal to co-attendance counts;
- (M5) a weighted 3-uniform hypergraph with unbounded count weights $|A_u \cap A_v \cap A_w|$;
- (M6) the pairwise fuzzy graph with Jaccard memberships $|A_u \cap A_v|/|A_u \cup A_v|$;
- (M7) the proposed fuzzy 3-uniform hypergraph.

Table 16 reports λ_2, $\lambda_{\max}$, the scale-free normalized gap $(n-1)\lambda_2/\operatorname{tr} L$ (equal to 1 exactly for 2-designs, by Theorem 6), the sizes of the two Fiedler groups, and the Rand index between each model's Fiedler partition and that of (M7).

Table 16 Alternative models of the Davis data. Norm. gap $= (n-1)\lambda_2/\operatorname{tr} L$; RI: Rand index with respect to the Fiedler partition of (M7).

Model	λ_2	$\lambda_{\max}$	Norm. gap	Fiedler groups	RI
(M1) Unweighted 3-uniform hypergraph (support of μ)	92.185	255.532	0.446	6/12	0.706
(M2) Crisp α-cut, $\alpha^* = 0.333$	0.961	44.142	0.043	3/15	0.529
(M3) Crisp α-cut, $\alpha = 0.5$	0.000	14.000	0.000	0/18	0.471
(M4) Weighted clique expansion of events (co-attendance counts)	12.757	62.330	0.337	2/16	0.497
(M5) Weighted 3-uniform hypergraph, $w(e) = \lvert A_u \cap A_v \cap A_w \rvert$	108.781	483.133	0.351	2/16	0.497
(M6) Pairwise fuzzy graph (Jaccard memberships)	2.021	6.948	0.388	8/10	0.889
(M7) Proposed fuzzy 3-uniform hypergraph L_μ	13.255	49.502	0.384	9/9	1.000

Three differences are mathematical rather than numerical.

1. The count-weighted models (M4) and (M5) produce a $2/16$ split. Their Fiedler vectors isolate the two least active women (Olivia and Flora, who attended only E9 and E11), because unbounded counts let the large events dominate. The bounded, normalized memberships of (M7) remove this activity bias and give a balanced $9/9$ split.
2. The crisp thresholds (M2) and (M3) either nearly disconnect the structure ($\lambda_2 = 0.96$) or disconnect it entirely ($\lambda_2 = 0$). This is the information loss that Theorem 5 avoids by averaging over levels.
3. The pairwise fuzzy graph (M6) agrees most closely with (M7) (Rand index 0.889), but it cannot express that a triad's cohesion is a joint property. Its memberships are pairwise, and the k-clique structure behind Theorems 2 and 15 is absent.

The models coincide in special cases: (M7) reduces to (M1) if all memberships are 1, and to a scaled (M1) if they are constant. Table 22 shows that (M6) is the case $k = 2$ of the same construction.

9.2 Tightness of Bounds and Certificates on Random Instances

For 492 random connected instances ($k \in \{3,4\}$, $n \le 12$, up to 40 hyperedges, three membership laws), we computed the ratio of each bound to the exact value; a ratio of 1 is ideal. Perturbations change 30% of the memberships by $\mathcal{N}(0, 0.1^2)$. Fractional certificates are evaluated at $\beta = 0.7$, $t = 5$.

The α-cut lower bound recovers on average 86% of λ_2, compared with 19% for the minimum-membership bound. Consequently, the α-cut fractional certificate is on average within 20% of the exact decay, whereas the minimum-membership certificate is on average 11 times too pessimistic. For $\lambda_{\max}$, the α-cut and $k d_{\max}$ bounds are much tighter than Gershgorin's. For perturbations, the load bound improves on Weyl by about 27% on average, and the Loewner bound improves on it further.

10 Statistical Validation and Performance Evaluation

The certificates of the framework are theorems, so they cannot fail. Their practical value, however, depends on how tight they are and on how stable the conclusions remain when the memberships are noisy. This section evaluates both

Table 17 Ratio of bound to exact value over 492 random instances (mean, median, minimum, maximum).

Quantity	Bound	Mean	Median	Min	Max
λ_2 (lower bounds; ideal $= 1$)	α-cut bound (Theorem 5)	0.855	0.875	0.400	0.987
	Minimum-membership bound	0.189	0.178	0.001	0.944
$\lambda_{\max}$ (upper bounds)	α-cut bound	1.068	1.057	1.004	1.301
	$k\,d_{\max}$ (Theorem 2)	1.181	1.170	1.046	1.339
	Gershgorin $2(k-1)d_{\max}$	1.670	1.678	1.459	1.809
Eigenvalue shift (upper bounds)	Loewner $\lambda_{\max}(L_{\lvert\delta\rvert})$	2.244	1.982	1.000	9.610
	Load $k\,\ell(\delta)$ (Theorem 7)	2.518	2.221	1.000	12.444
	Weyl $k\lVert\delta\rVert_1$	3.457	3.149	1.000	16.317
Decay certificate, $\beta = 0.7$, $t = 5$	α-cut certificate	1.198	1.150	1.002	2.740
	Minimum-membership certificate	11.198	6.083	1.002	164.489

aspects by repeated perturbation trials on the two case studies, using descriptive statistics together with parametric and non-parametric tests.

10.1 Experimental Design and Definition of Observations

A single observation corresponds to one execution of the diagnostic phases of Algorithm 1 (Phases 2 and 3) on a perturbed membership function. In trial j, every membership is perturbed independently by up to 10%,

$$\nu^{(j)}(e) = \min\bigl\{1,\ \mu(e)\,(1+0.1\,u_e^{(j)})\bigr\}, \qquad u_e^{(j)} \sim U(-1,1),$$

and the following quantities are recorded: the algebraic connectivity $\lambda_2(L_{\nu^{(j)}})$; the tightness ratios $\rho_\alpha = \gamma_\alpha/\lambda_2$ of the α-cut certificate and $\rho_{\min} = \nu_{\min}\lambda_2(L(H))/\lambda_2$ of the minimum-membership certificate (a value of 1 means an exact certificate); and the overestimation factors of three perturbation bounds, namely the Loewner bound $\lambda_{\max}(L_{\lvert\delta\rvert})$, the load bound $k\,\ell(\delta)$ and the Weyl bound $k\lVert\delta\rVert_1$, each divided by the observed spectral shift. The process is repeated over $N = 100$ independent trials per dataset. Table 18 lists the parameter settings.

Table 18 Key parameter settings used in the case studies and in the statistical validation.

Parameter	Symbol	Davis data	High-school data
Number of actors (vertices)	n	18	317
Uniformity	k	3	3
Number of fuzzy hyperedges	m	586	2370
Total membership (budget)	W	97.692	40.355
Fractional orders	β	0.4, 0.6, 0.8, 1.0	
Settling tolerance	ε	0.1	
Super-gradient iterations	T	3000	12000
Perturbation amplitude		10%	
Number of perturbation trials	N	100	

10.2 Preliminary Data Validation

Before the trials, every identity and inequality of Sections 3–5 was checked on 3000 random instances (spectral results) and 300 random instances (fractional results); the largest violation was 2.3×10^{-13}, which is floating-point rounding, and the closed-form fractional solution agreed with an independent L1 finite-difference scheme to 1.9×10^{-4}. The verification scripts are part of the Supplementary Material. In all 200 trials every theoretical inequality held ($\gamma_\alpha \le \lambda_2$, minimum-membership bound $\le \gamma_\alpha$, and observed shift $\le$ Loewner $\le$ load $\le$ Weyl), with no violation. The Shapiro–Wilk test does not reject normality of λ_2 for the Davis data ($W = 0.989$, $p = 0.61$) but rejects it at the 5% level for the high-school data ($W = 0.971$, $p = 0.027$). Non-parametric tests are therefore used for all comparisons.

10.3 Stability and Tightness of the Certificates

Table 19 reports the results. The algebraic connectivity is stable under 10% membership noise: its coefficient of variation is 0.43% for the Davis data and 1.13% for the high-school data. The α-cut certificate recovers on average 88.8% of the

exact value for the Davis data and 39.3% for the high-school data, against 45.3% and 14.4% for the minimum-membership certificate, and its tightness is itself stable (standard deviations 0.003 and 0.014).

Table 19 Stability of λ_2 and tightness of the certificates over $N = 100$ perturbation trials (mean $\pm$ standard deviation). CV: coefficient of variation. Wins: trials in which $\rho_\alpha > \rho_{\min}$.

Dataset	Mean λ_2	SD	CV (%)	ρ_α	$\rho_{\min}$	Wins
Davis ($n = 18$)	13.25957	0.05756	0.43	0.888 ± 0.003	0.453 ± 0.005	100/100
High school ($n = 317$)	0.00955	0.00011	1.13	0.393 ± 0.014	0.144 ± 0.006	100/100

10.4 Pairwise and Multiple-Comparison Testing

A one-sided Wilcoxon signed-rank test of ρ_α against $\rho_{\min}$ gives the maximal statistic $W^+ = 5050$ ($p = 1.9 \times 10^{-18}$) for both datasets, since the α-cut certificate is tighter in every trial. Table 20 compares the three perturbation bounds. The Friedman test gives $\chi^2 = 200$ ($p = 3.7 \times 10^{-44}$) for both datasets, with mean ranks 1, 2 and 3 for the Loewner, load and Weyl bounds. These orderings are guaranteed by Theorems 5 and 7, so the tests confirm the theory rather than discover the ordering; the informative quantities are the effect sizes. For dispersed noise, the load bound overestimates the observed shift by a factor of 9.7 (Davis) and 2.1 (high school), whereas the Weyl bound overestimates it by factors of 40 and 61. The advantage of the load bound thus grows with the size of the system, from a factor of about 4 to a factor of about 30.

Table 20 Overestimation factors (bound divided by observed spectral shift; mean $\pm$ standard deviation over $N = 100$ trials) and Friedman statistic.

Dataset	Loewner	Load	Weyl	Friedman χ^2
Davis ($n = 18$)	7.02 ± 2.22	9.68 ± 3.06	40.1 ± 12.6	200.0
High school ($n = 317$)	1.86 ± 0.47	2.07 ± 0.54	61.1 ± 16.9	200.0

10.5 Scope of the Validation

The validation concerns the tightness and stability of the certificates. It does not measure predictive accuracy against observed opinion trajectories, because neither dataset records opinions over time.

11 Sensitivity Analysis of the FFHC Results

11.1 Fractional Order

Table 21 reports, for the Davis hypergraph, the observed disagreement ratio $\|e(t)\|/\|e(0)\|$ of the trajectory from the participation-rate initial state, together with the worst-case value $E_\beta(-\lambda_2 t^\beta)$ in parentheses and the exact settling times for $\varepsilon = 0.1$ and $\varepsilon = 0.01$.

Table 21 Sensitivity to the fractional order β (Davis data): observed ratio (worst case in parentheses) and settling times.

β	$t = 0.05$	$t = 0.2$	$t = 1$	$t = 5$	$T_{0.1}$	$T_{0.01}$
0.2	0.0635	0.0490	0.0361	0.0265	0.0705	10917.057
	(0.1064)	(0.0826)	(0.0612)	(0.0450)		
0.4	0.0911	0.0540	0.0289	0.0153	0.1582	57.065
	(0.1526)	(0.0916)	(0.0494)	(0.0263)		
0.6	0.1260	0.0544	0.0202	0.0076	0.1816	7.798
	(0.2159)	(0.0942)	(0.0349)	(0.0131)		
0.8	0.1828	0.0468	0.0103	0.0027	0.1750	1.995
	(0.3279)	(0.0868)	(0.0181)	(0.0047)		
1.0	0.2965	0.0306	0.0000	0.0000	0.1737	0.347
	(0.5154)	(0.0706)	(0.0000)	(0.0000)		

The order β changes the shape of convergence and not merely its speed. At early times ($t = 0.05$), smaller β produces *faster* alignment, because $t^\beta > t$ for $t < 1$. At later times the ordering reverses, and reaching 1% disagreement takes 0.35

time units for $\beta = 1$ but about 10^4 for $\beta = 0.2$. In every case the observed trajectory respects the worst-case bound of Theorem 11.

11.2 Data Perturbations and Membership Revisions

Table 8 is itself a sensitivity analysis with respect to the data: the spectrum is stable under the deletion of any small event, and sensitive only to the two largest events. Table 10 gives the full range induced by single-event uncertainty.

11.3 Uniformity Parameter

Table 22 repeats the construction (15) with groups of size $k = 2$ (pairs, i.e., model (M6)), $k = 3$ and $k = 4$.

Table 22 Sensitivity to the uniformity parameter k (Davis data). RI with respect to the $k = 3$ Fiedler partition.

k	m	W	λ_2	$\lambda_{\max}$	Norm. gap	RI
2	139	44.33	2.021	6.948	0.388	0.889
3	586	97.69	13.255	49.502	0.384	1.000
4	1567	182.58	38.763	188.645	0.301	0.575

The partitions for $k = 2$ and $k = 3$ largely agree (RI 0.889). For $k = 4$ the agreement drops (RI 0.575), plausibly because co-attending quadruples are dominated by the large events E7–E9, which are attended by women from both groups. The choice $k = 3$ is the smallest genuinely higher-order unit, and we regard it as the natural default.

11.4 Budget

Table 12 shows that the gain of the optimal fuzzy allocation over the rescaled observed memberships is stable across budgets: the ratio lies between 2.22 and 2.27. The best random crisp allocations fall far below the fuzzy optimum at small budgets (0.53 versus 3.08 at $W = 10$).

12 Discussion: Advantages and Limitations

12.1 Advantages

- The framework links the defining features of fuzzy information (α-cuts, bounded memberships, interval uncertainty) to rigorous spectral statements, and through the Mittag-Leffler function to fractional dynamics with memory.
- The α-cut certificates are computable and tight in practice (Tables 11 and 17), and much sharper than minimum-membership transfers.
- The stability results distinguish localized from dispersed revisions and losses from gains, and they provide exact interval ranges. On real data, they certify robustness where Weyl-type bounds give no guarantee, and they are up to 18 times sharper than Weyl-type bounds.
- The optimal-allocation results hold simultaneously for all fractional orders, are accompanied by computable optimality certificates, and identify when graded memberships are strictly better than crisp ones.
- All computations are polynomial apart from optional validation searches, and they are fully reproducible.

12.2 Limitations

- The Laplacian depends on memberships only through fuzzy codegrees. Hypergraphs with equal codegree matrices (e.g., non-isomorphic 2-designs with the same parameters) cannot be distinguished; tensor approaches [19, 20] can, at higher computational cost.
- The fractional model is linear and uses a single order β for all agents; heterogeneous or distributed orders are not covered.
- The spectral-radius problem $(\mathrm{P}_{\max})$ is solved exactly only in the extremal regime of Theorem 15; otherwise extreme-point search or local search is needed.
- The applications use co-attendance and co-presence as memberships. They involve at most 317 actors, and the dynamic model is illustrative rather than empirically validated, because neither dataset records opinions over time.

13 Conclusion and Future Research Directions

This study introduced the FFHC framework as a unified mathematical model for uncertain group interactions whose collective dynamics carry memory. By combining the graded memberships of fuzzy sets, the higher-order structure of uniform hypergraphs and the memory-preserving behaviour of the Caputo derivative, the proposed model bridges a gap in the existing literature, where fuzzy graph and hypergraph models are static and consensus models ignore the level structure of fuzzy information. The framework overcomes these limitations through the spectral theory of the fuzzy Laplacian: an exact α-cut resolution, sharp spectral-radius bounds, localized, one-sided and interval-valued stability results, two-sided Mittag-Leffler decay bounds and a characterization of optimal membership allocations. A key contribution is the SPEC-FC algorithm, which turns these results into consensus-speed certificates, robustness ranges and certified-optimal allocations. The empirical evaluation on two real social systems demonstrates the practical value of the approach. On the Davis data, the one-sided certificate guarantees that cohesion survives the loss of any of 12 of the 14 events, whereas the Weyl bound certifies none, and the α-cut certificates lie within 13–35% of the exact settling times. On the high-school contact data, every crisp threshold above 0.0032 disconnects the structure while the fuzzy model remains connected; the optimal allocation, certified within 0.64% of optimality, raises the algebraic connectivity by a factor of 12.3, whereas no crisp allocation within the same budget can connect the students. Over 100 perturbation trials per dataset, the algebraic connectivity varied by at most 1.13% (coefficient of variation) under 10% membership noise, the α-cut certificate was tighter than the minimum-membership certificate in every trial, and the load bound was between 4 and 30 times sharper than the Weyl bound. Not every finding is favourable: in the larger system no recording day is dispensable, and the framework reports this exactly instead of issuing a false guarantee. These results position graded memberships as more than a descriptive refinement. They are what makes consensus possible, certifiable and optimizable in the systems studied.

Future research directions. Building on the foundations established in this work, several research avenues emerge naturally:

- **Non-uniform and incidence-fuzzy hypergraphs:** extending the theory to hyperedges of mixed sizes and to fuzzy vertex–hyperedge incidences.
- **Heterogeneous memory:** distributed-order, variable-order and agent-dependent fractional consensus on fuzzy hypergraphs.
- **Tensor-based fuzzy Laplacians:** distinguishing hypergraphs with equal codegrees, at higher computational cost.
- **Scalable implementations:** sparse eigensolvers and first-order semidefinite methods for systems with thousands of actors.
- **Learning the memberships:** estimating membership degrees and the fractional order from data by neural or evolutionary methods, with the certificates of this paper as constraints.
- **Broadening empirical applications:** validating the dynamics on datasets that record opinions over time, and applying the framework to committee, co-authorship and communication data.

In summary, the proposed framework provides a mathematically rigorous and practically usable tool for analysing uncertain higher-order systems. Its certificates are computable, its conclusions are stable under noise, and its limitations are explicit, which makes it a sound basis for further fuzzy and fractional models of group decision processes.

Acknowledgements Not applicable.

Author Contributions Conceptualization: A.S.; Methodology: A.S.; Formal analysis: A.S.; Investigation: A.S.; Validation: A.M.A.; Data curation: A.M.A.; Writing – original draft: A.S.; Project administration: A.M.A. All authors read and approved the final manuscript.

Funding No funding was received for this study.

Data Availability All data analysed for this article are publicly available. The Davis data are distributed with the Python library NetworkX (function `davis_southern_women_graph`). The high-school contact data [11] are available in the timestamped-simplex form of [40] at https://github.com/arbenson/ScHoLP-Data. The code that reproduces all results is provided as Supplementary Material.

Competing Interests The authors declare no competing interests.

References

1. Battiston, F., Cencetti, G., Iacopini, I., Latora, V., Lucas, M., Patania, A., Young, J.-G., Petri, G.: Networks beyond pairwise interactions: Structure and dynamics. Phys. Rep. **874**, 1–92 (2020) https://doi.org/10.1016/j.physrep.2020.05.004

2. Zadeh, L.A.: Fuzzy sets. Inf. Control **8**, 338–353 (1965) https://doi.org/10.1016/S0019-9958(65)90241-X
3. Goetschel, R.H.: Introduction to fuzzy hypergraphs and Hebbian structures. Fuzzy Sets Syst. **76**, 113–130 (1995) https://doi.org/10.1016/0165-0114(94)00381-G
4. Gong, S., Hua, G., Gao, W.: Domination of bipolar fuzzy graphs in various settings. Int. J. Comput. Intell. Syst. **14**, 162 (2021) https://doi.org/10.1007/s44196-021-00011-2
5. Shi, X., Kosari, S., Talebi, A.A., Sadati, S.H., Rashmanlou, H.: Investigation of the main energies of picture fuzzy graph and its applications. Int. J. Comput. Intell. Syst. **15**, 31 (2022) https://doi.org/10.1007/s44196-022-00086-5
6. Shaik, N., Shaik, S.B.: Similarity measures and energy-based decision-making in intuitionistic fuzzy rough graphs. Int. J. Comput. Intell. Syst. **19**, 120 (2026) https://doi.org/10.1007/s44196-026-01195-1
7. Cao, Y., Li, Y., Ren, W., Chen, Y.: Distributed coordination of networked fractional-order systems. IEEE Trans. Syst. Man Cybern. Part B Cybern. **40**, 362–370 (2010) https://doi.org/10.1109/TSMCB.2009.2024647
8. Mainardi, F.: On some properties of the Mittag-Leffler function $E_\alpha(-t^\alpha)$, completely monotone for $t > 0$ with $0 < \alpha < 1$. Discrete Contin. Dyn. Syst. Ser. B **19**, 2267–2278 (2014) https://doi.org/10.3934/dcdsb.2014.19.2267
9. Rodríguez, J.A.: On the Laplacian eigenvalues and metric parameters of hypergraphs. Linear Multilinear Algebra **50**, 1–14 (2002) https://doi.org/10.1080/03081080290011692
10. Rodríguez, J.A.: Laplacian eigenvalues and partition problems in hypergraphs. Appl. Math. Lett. **22**, 916–921 (2009) https://doi.org/10.1016/j.aml.2008.07.020
11. Mastrandrea, R., Fournet, J., Barrat, A.: Contact patterns in a high school: A comparison between data collected using wearable sensors, contact diaries and friendship surveys. PLoS ONE **10**(9), 0136497 (2015) https://doi.org/10.1371/journal.pone.0136497
12. Luqman, A., Akram, M., Al-Kenani, A.N.: q-rung orthopair fuzzy hypergraphs with applications. Mathematics **7**, 260 (2019) https://doi.org/10.3390/math7030260
13. Sarwar, M., Akram, M., Alshehri, N.O.: A new method to decision-making with fuzzy competition hypergraphs. Symmetry **10**, 404 (2018) https://doi.org/10.3390/sym10090404
14. Akram, M., Shahzadi, S., Rasool, A., Sarwar, M.: Decision-making methods based on fuzzy soft competition hypergraphs. Complex Intell. Syst. **8**, 2325–2348 (2022) https://doi.org/10.1007/s40747-022-00646-4
15. Pramanik, T., Mahapatra, R., Allahviranloo, T., Mrsic, L., Kalampakas, A., Samanta, S.: Spherical fuzzy hypergraph in decision making. Sci. Rep. **16**, 14577 (2026) https://doi.org/10.1038/s41598-026-44917-3
16. Gutman, I., Zhou, B.: Laplacian energy of a graph. Linear Algebra Appl. **414**, 29–37 (2006) https://doi.org/10.1016/j.laa.2005.09.008
17. Rodríguez, J.A.: On the Laplacian spectrum and walk-regular hypergraphs. Linear Multilinear Algebra **51**, 285–297 (2003) https://doi.org/10.1080/0308108031000084374
18. Banerjee, A.: On the spectrum of hypergraphs. Linear Algebra Appl. **614**, 82–110 (2021) https://doi.org/10.1016/j.laa.2020.01.012
19. Cooper, J., Dutle, A.: Spectra of uniform hypergraphs. Linear Algebra Appl. **436**, 3268–3292 (2012) https://doi.org/10.1016/j.laa.2011.11.018
20. Qi, L.: H^+-eigenvalues of Laplacian and signless Laplacian tensors. Commun. Math. Sci. **12**, 1045–1064 (2014) https://doi.org/10.4310/CMS.2014.v12.n6.a3
21. Hu, S., Qi, L.: The Laplacian of a uniform hypergraph. J. Comb. Optim. **29**, 331–366 (2015) https://doi.org/10.1007/s10878-013-9596-x
22. Chan, T.-H.H., Louis, A., Tang, Z.G., Zhang, C.: Spectral properties of hypergraph Laplacian and approximation algorithms. J. ACM **65**, 1–48 (2018) https://doi.org/10.1145/3178123
23. Carletti, T., Battiston, F., Cencetti, G., Fanelli, D.: Random walks on hypergraphs. Phys. Rev. E **101**, 022308 (2020) https://doi.org/10.1103/PhysRevE.101.022308
24. Antelmi, A., Cordasco, G., Polato, M., Scarano, V., Spagnuolo, C., Yang, D.: A survey on hypergraph representation learning. ACM Comput. Surv. **56**, 1–38 (2024) https://doi.org/10.1145/3605776
25. Tang, Z., Hao, T., Cheng, D., Cheng, F.: Trust improvement consensus model considering unreliability degree of opinions with hesitant fuzzy sets. Int. J. Comput. Intell. Syst. **17**, 116 (2024) https://doi.org/10.1007/s44196-024-00507-7
26. Pollard, H.: The completely monotonic character of the Mittag-Leffler function $E_a(-x)$. Bull. Am. Math. Soc. **54**, 1115–1116 (1948) https://doi.org/10.1090/S0002-9904-1948-09132-7
27. Simon, T.: Comparing Fréchet and positive stable laws. Electron. J. Probab. **19**, 1–25 (2014) https://doi.org/10.1214/EJP.v19-3058
28. Garrappa, R.: Numerical evaluation of two and three parameter Mittag-Leffler functions. SIAM J. Numer. Anal. **53**, 1350–1369 (2015) https://doi.org/10.1137/140971191
29. Fiedler, M.: Algebraic connectivity of graphs. Czechoslov. Math. J. **23**, 298–305 (1973) https://doi.org/10.21136/CMJ.1973.101168

30. Abreu, N.M.M.: Old and new results on algebraic connectivity of graphs. Linear Algebra Appl. **423**, 53–73 (2007) https://doi.org/10.1016/j.laa.2006.08.017

31. Shakeri, H., Albin, N., Darabi Sahneh, F., Poggi-Corradini, P., Scoglio, C.: Maximizing algebraic connectivity in interconnected networks. Phys. Rev. E **93**, 030301 (2016) https://doi.org/10.1103/PhysRevE.93.030301

32. Somisetty, N., Nagarajan, H., Darbha, S.: Optimal robust network design: Formulations and algorithms for maximizing algebraic connectivity. IEEE Trans. Control Netw. Syst. **12**, 918–929 (2025) https://doi.org/10.1109/TCNS.2024.3431408

33. Wang, X., Ma, W., Zou, J.: Synchronization of short-memory fractional directed higher-order networks. Fractal Fract. **9**, 440 (2025) https://doi.org/10.3390/fractalfract9070440

34. Zadeh, L.A.: Similarity relations and fuzzy orderings. Inf. Sci. **3**, 177–200 (1971) https://doi.org/10.1016/S0020-0255(71)80005-1

35. Gorzałczany, M.B.: A method of inference in approximate reasoning based on interval-valued fuzzy sets. Fuzzy Sets Syst. **21**, 1–17 (1987) https://doi.org/10.1016/0165-0114(87)90148-5

36. Atanassov, K.T.: Intuitionistic fuzzy sets. Fuzzy Sets Syst. **20**, 87–96 (1986) https://doi.org/10.1016/S0165-0114(86)80034-3

37. Weyl, H.: Das asymptotische Verteilungsgesetz der Eigenwerte linearer partieller Differentialgleichungen (mit einer Anwendung auf die Theorie der Hohlraumstrahlung). Math. Ann. **71**, 441–479 (1912) https://doi.org/10.1007/BF01456804

38. Fan, K.: On a theorem of Weyl concerning eigenvalues of linear transformations I. Proc. Natl. Acad. Sci. USA **35**, 652–655 (1949) https://doi.org/10.1073/pnas.35.11.652

39. Hertz, D.: The extreme eigenvalues and stability of real symmetric interval matrices. IEEE Trans. Autom. Control **37**, 532–535 (1992) https://doi.org/10.1109/9.126593

40. Benson, A.R., Abebe, R., Schaub, M.T., Jadbabaie, A., Kleinberg, J.: Simplicial closure and higher-order link prediction. Proc. Natl. Acad. Sci. USA **115**(48), 11221–11230 (2018) https://doi.org/10.1073/pnas.1800683115

Authors and Affiliations

Abdulkafi Sanad
abdulkafisanad@stu.ynu.edu.cn

Alhanouf M. Almutairi
ammutairi@uqu.edu.sa

[1] School of Mathematics and Statistics, Yunnan University, Kunming 650500, China

[2] Department of Mathematics, Adham University College, Umm Al-Qura University, Makkah 21955, Saudi Arabia